

PARAXIAL WAVE PROPAGATION IN RANDOM MEDIA WITH LONG-RANGE CORRELATIONS

LILIANA BORCEA*, JOSSELIN GARNIER†, AND KNUT SØLNA‡

Abstract. We study the paraxial wave equation with a randomly perturbed index of refraction, which can model the propagation of a wave beam in a turbulent medium. The random perturbation is a stationary and isotropic process with a general form of the covariance that may be integrable or not. We focus attention mostly on the non-integrable case, which corresponds to a random perturbation with long-range correlations, that is relevant for propagation through a cloudy turbulent atmosphere. The analysis is carried out in a high-frequency regime where the forward scattering approximation holds. It reveals that the randomization of the wave field is multiscale: The travel time of the wave front is randomized at short distances of propagation and it can be described by a fractional Brownian motion. The wave field observed in the random travel time frame is affected by the random perturbations at long distances, and it is described by a Schrödinger-type equation driven by a standard Brownian field. We use these results to quantify how scattering leads to decorrelation of the spatial and spectral components of the wave field and to a deformation of the pulse emitted by the source. These are important questions for applications like imaging and free space communications with pulsed laser beams through a turbulent atmosphere. We also compare the results with those used in the optics literature, which are based on the Kolmogorov model of turbulence.

Key words. Paraxial wave equation, turbulent atmosphere, asymptotic analysis, long-range correlations.

AMS subject classifications. 76B15, 35Q94, 60F05.

1. Introduction. The paraxial wave equation describes wave propagation along a privileged axis, as a narrow angle beam, in a homogeneous or heterogeneous medium [3]. It is a parabolic approximation of the wave equation, which neglects backscattering and thus facilitates the analysis and computation of waves at long distance of propagation, aka range. The parabolic approximation theory was introduced by Levontovich and Fock [26] and has been used and developed further in applied fields like seismology [12, 13], underwater acoustics [33], optics [22] and laser optics [1, 23, 34, 35].

Motivated by laser optics applications to imaging and free space communications through a turbulent atmosphere, we consider the paraxial wave equation with a randomly perturbed wave speed $c(\vec{x})$. The model of the perturbation is

$$\frac{c_o^2}{c^2(\vec{x})} = 1 + \mu(\vec{x}), \quad (1.1)$$

where c_o is the constant reference speed and μ is a zero-mean, stationary and isotropic random process, with power spectral density (Fourier transform of the covariance) of the form

$$\mathbb{S}(\vec{\kappa}) = \int_{\mathbb{R}^3} d\vec{x} \mathbb{E} [\mu(\vec{x}') \mu(\vec{x}' + \vec{x})] e^{-i\vec{\kappa} \cdot \vec{x}} = \chi_\alpha \mathbf{1}_{(L_o^{-1}, l_o^{-1})}(|\vec{\kappa}|) |\vec{\kappa}|^{-2-\alpha}. \quad (1.2)$$

Here χ_α is a constant (expressed in unit of length to the power $1-\alpha$), $\alpha \in (0, 1) \cup (1, 2)$ and $\mathbf{1}_{(L_o^{-1}, l_o^{-1})}$ is the indicator function equal to one when its argument is in (L_o^{-1}, l_o^{-1}) and zero otherwise.

*Department of Mathematics, University of Michigan, Ann Arbor, MI 48109. borcea@umich.edu

†Centre de Mathématiques Appliquées, Ecole Polytechnique, Institut Polytechnique de Paris, 91128 Palaiseau Cedex, France. josselin.garnier@polytechnique.edu

‡Department of Mathematics, University of California at Irvine, Irvine, CA 92697. ksolna@math.uci.edu

Definition (1.2) is a generalization of the commonly used Kolmogorov power spectrum, where $\alpha = 5/3$ and the “outer scale” L_o and the “inner scale” l_o define the “inertial range” of turbulence [1]. There is a growing number of studies in the optics literature concerned with quantifying the effect of non-Kolmogorov turbulence on beam propagation [11, 24, 36]. All of them consider $\alpha > 1$, which corresponds to an integrable covariance of μ . This case is well understood from the mathematical point of view and has been analyzed in detail in the high-frequency, paraxial regime in [14, 16]. The wave field is described asymptotically by the solution of an Itô-Schrödinger equation driven by a Brownian field with covariance defined in terms of $\mathbb{S}(\vec{\kappa})$. Therefore, the second and even fourth order statistical moments of the wave field can be calculated using Itô calculus [17]. The study of such moments is an essential part of both the analysis and the development of new methodologies for imaging [5, 9, 18], time reversal [4, 15, 19, 31] and optical communications applications [7].

The case $\alpha \in (0, 1)$ has not been explored in the optics literature and it is interesting mathematically because depending on the outer scale L_o , it may give a non-integrable covariance of the fluctuations, meaning that μ has long-range correlations. Moreover, $\alpha < 1$ is relevant for propagation through a cloudy atmosphere, as seen from the experimental studies [10] and [27, Table 3]. The conclusion of these studies is that the value of α depends on the interval (L_o^{-1}, l_o^{-1}) , with $\alpha < 1$ at length scales that are larger than the outer scale of Kolmogorov turbulence. Thus, one could consider an even more general model of the power spectrum, with $\alpha < 1$ at longer scales and $\alpha > 1$ at smaller scales. For brevity, we work with the model (1.2), which is sufficient to display the effects of long range medium fluctuations on the statistics of the wave beam.

Most of our analysis is concerned with $\alpha \in (0, 1)$ and a beam with initial radius of order r_s , satisfying $l_o \lesssim r_s \ll L_o$, so we can take $L_o \rightarrow \infty$, while keeping l_o finite. The covariance of μ is non-integrable in this case, which means that the classic paraxial theory in [14, 16] does not apply. We refer to [20] for the derivation of the paraxial approximation in a random anisotropic medium with long-range correlation properties. There, the wave is described asymptotically by the solution of a Schrödinger equation with fractional white noise potential. In this paper we show that for our isotropic random medium modeled by μ , a transformation involving the central axis travel time (i.e., the travel time measured at the center of the beam), can convert the problem to one where the classic analytic framework applies. We prove that there are two distinguished range scales that describe the net scattering effects on the beam: The central axis travel time randomizes on a small range scale and it is described by a fractional Brownian motion. This behavior was also shown in [2, 32]. The shape of the wave, observed in the random travel time frame, is not affected by scattering at this short range. However, this, too, randomizes at long range and it is described by the solution of an Itô-Schrödinger equation driven by a standard Brownian field, like in [14, 16]. We use these asymptotic results to analyze explicitly the spatial and frequency covariance of the wave field. This allows us to quantify how the wave components decorrelate and how the pulse emitted by the source deforms due to scattering in the random medium.

To relate our results with the existing optics literature, we also consider briefly the case $\alpha \in (0, 1) \cup (1, 2)$ with a finite L_o . These cases correspond to an integrable covariance of the process μ , where the theory in [14, 16] applies. We study the covariance of the wave field, which depends on α and the scales l_o and L_o , and quantify explicitly the accuracy of the approximations commonly used in optics literature [1].

The paper is organized as follows: We begin in section 2 with the mathematical formulation of the problem. We state the paraxial wave equation, identify the asymptotic regime and give more details on the random process μ . The asymptotic analysis for the case $\alpha \in (0, 1)$, with $L_o \rightarrow \infty$ and finite l_o is given in section 3. We use it in section 4 to quantify the decorrelation of the wave components and the deformation of the pulse due to scattering. The comparison with the formulas in the optics literature are in section 5. We end with a summary in section 6.

2. Mathematical formulation. Let us introduce the orthogonal system of coordinates $\vec{\mathbf{x}} = (\mathbf{x}, z)$, with range axis z along the direction of propagation and with $\mathbf{x} \in \mathbb{R}^2$ in the cross-range plane. The wave field u satisfies the wave equation

$$\left[\frac{1}{c^2(\mathbf{x}, z)} \partial_t^2 - \Delta_{\mathbf{x}} - \partial_z^2 \right] u(t, \mathbf{x}, z) = \partial_t [2 \cos(\omega_o t) f(Bt)] S\left(\frac{\mathbf{x}}{r_s}\right) \delta(z), \quad (2.1)$$

for $(t, \mathbf{x}, z) \in \mathbb{R} \times \mathbb{R}^2 \times \mathbb{R}$, where $\Delta_{\mathbf{x}}$ denotes the Laplacian with respect to \mathbf{x} . The source is localized at the origin of range and has a cross-range profile with radius r_s , modeled by the function S of dimensionless argument, with support centered at $\mathbf{0}$. The source signal is a pulse with bandwidth B , modulated at the carrier (center) frequency ω_o and with envelope modeled by the function f of dimensionless argument. Prior to the source excitation there is no wave: $u(t, \mathbf{x}, z) \equiv 0$, for $t \ll -1/B$.

Since the analysis of wave propagation requires the decomposition of the wave field over frequencies, we work henceforth in the Fourier domain,

$$\hat{u}(\omega, \mathbf{x}, z) = \int_{-\infty}^{\infty} dt e^{i\omega t} u(t, \mathbf{x}, z). \quad (2.2)$$

This time-harmonic wave satisfies the Helmholtz equation

$$\left[\frac{\omega^2}{c^2(\mathbf{x}, z)} + \Delta_{\mathbf{x}} + \partial_z^2 \right] \hat{u}(\omega, \mathbf{x}, z) = i\omega \hat{F}(\omega, \mathbf{x}) \delta(z), \quad (2.3)$$

for $(\omega, \mathbf{x}, z) \in \mathbb{R} \times \mathbb{R}^2 \times \mathbb{R}$, with

$$\hat{F}(\omega, \mathbf{x}) = \frac{1}{B} \left[\hat{f}\left(\frac{\omega - \omega_o}{B}\right) + \hat{f}\left(\frac{\omega + \omega_o}{B}\right) \right] S\left(\frac{\mathbf{x}}{r_s}\right), \quad (2.4)$$

and outgoing boundary conditions at $|(\mathbf{x}, z)| \rightarrow \infty$. These conditions can be justified mathematically by truncating the random medium outside a ball of large enough radius, so that in the time domain, the truncation does not affect the wave over the duration of interest.

We state next, in subsection 2.1, the paraxial approximation of equation (2.3) and the asymptotic regime where it is valid. The details on the random process μ are in subsection 2.2.

2.1. Scaling and the paraxial equation. The paraxial approximation holds in a high-frequency regime, where the wavelength is much smaller than the radius of the beam and the correlation radius of the medium, which are, in turn, much smaller than the range scale (distance of propagation).

We introduce the small dimensionless parameter $\varepsilon > 0$ that encapsulates this regime and assume that, compared to the typical range, the typical wavelength is of order ε^4 and the beam radius and the correlation radius are of order ε^2 :

$$B^\varepsilon = \frac{B}{\varepsilon^4}, \quad \omega_o^\varepsilon = \frac{\omega_o}{\varepsilon^4}, \quad r_s^\varepsilon = \varepsilon^2 r_s, \quad l_o^\varepsilon = \varepsilon^2 l_o, \quad L_o^\varepsilon = \varepsilon^2 L_o, \quad \chi_\alpha^\varepsilon = \chi_\alpha \varepsilon^{8-2\alpha}. \quad (2.5)$$

As we will see, the scaling of χ_α^ε is the one that gives a non-trivial limit as $\varepsilon \rightarrow 0$. It is also possible to consider a larger range scale $L_o^\varepsilon = \varepsilon^p L_o$, with $p < 2$, and/or a smaller $l_o^\varepsilon = \varepsilon^q l_o$, with $q > 2$ [14]. Here we consider the scaling (2.5) and study the subsequent limits $L_o \rightarrow +\infty$ and/or $l_o \rightarrow 0$.

We denote by μ^ε a random process with the power spectral density of the form (1.2) with the constant χ_α^ε and scales $l_o^\varepsilon, L_o^\varepsilon$. Then, (2.5) gives the representation

$$\mu^\varepsilon(\vec{\mathbf{x}}) = \varepsilon^3 \mu\left(\frac{\vec{\mathbf{x}}}{\varepsilon^2}\right), \quad (2.6)$$

where μ is a random process with the power spectral density of the form (1.2) with the constant χ_α and scales l_o, L_o . The wave field in the scaling (2.5) is denoted by \hat{u}^ε and it satisfies the following Helmholtz equation derived from (2.3)

$$\left[\frac{\omega^2}{c_o^2} [1 + \mu^\varepsilon(\mathbf{x}, z)] + \Delta_{\mathbf{x}} + \partial_z^2 \right] \hat{u}^\varepsilon(\omega, \mathbf{x}, z) = i\omega \hat{F}^\varepsilon(\omega, \mathbf{x}) \delta(z), \quad (2.7)$$

with

$$\hat{F}^\varepsilon(\omega, \mathbf{x}) = \frac{1}{B^\varepsilon} \left[\hat{f}\left(\frac{\omega - \omega_o^\varepsilon}{B^\varepsilon}\right) + \hat{f}\left(\frac{\omega + \omega_o^\varepsilon}{B^\varepsilon}\right) \right] S\left(\frac{\mathbf{x}}{r_s^\varepsilon}\right) = \varepsilon^4 \hat{F}\left(\varepsilon^4 \omega, \frac{\mathbf{x}}{\varepsilon^2}\right), \quad (2.8)$$

and outgoing boundary conditions at $|\mathbf{x}, z| \rightarrow \infty$.

Observe that if we had $S \equiv 1$ and $\mu \equiv 0$ in (2.7-2.8), the solution would be the plane wave

$$\hat{u}^\varepsilon(\omega, \mathbf{x}, z) = \frac{c_o \varepsilon^4}{2} \exp\left(i \frac{\omega}{c_o} z\right) \frac{1}{B} \left[\hat{f}\left(\frac{\varepsilon^4 \omega - \omega_o}{B}\right) + \hat{f}\left(\frac{\varepsilon^4 \omega + \omega_o}{B}\right) \right].$$

This observation motivates the introduction of the ‘‘slowly varying envelope field’’ φ^ε , which defines the solution of (2.7-2.8) as follows

$$\hat{u}^\varepsilon(\omega, \mathbf{x}, z) = \frac{c_o \varepsilon^4}{2} \exp\left(i \frac{\omega}{c_o} z\right) \varphi^\varepsilon\left(\varepsilon^4 \omega, \frac{\mathbf{x}}{\varepsilon^2}, z\right). \quad (2.9)$$

Substituting (2.9) into (2.7), using the chain rule and denoting $k(\Omega) = \Omega/c_o$, we find that for $\Omega = \varepsilon^4 \omega \in \mathbb{R}$ and $\mathbf{X} = \mathbf{x}/\varepsilon^2 \in \mathbb{R}^2$, we have

$$\left[2ik(\Omega)\partial_z + \Delta_{\mathbf{X}} + \frac{k^2(\Omega)}{\varepsilon} \mu\left(\mathbf{X}, \frac{z}{\varepsilon^2}\right) \right] \varphi^\varepsilon(\Omega, \mathbf{X}, z) = 0, \quad z > 0, \quad (2.10)$$

$$\varphi^\varepsilon(\Omega, \mathbf{X}, z = 0) = \hat{F}(\Omega, \mathbf{X}). \quad (2.11)$$

In equation (2.10) we have neglected the $\varepsilon^4 \partial_z^2 \varphi^\varepsilon$ term, which is responsible for backscattering. Thus, we use the forward scattering approximation, which can be justified when $\varepsilon \rightarrow 0$ as shown in [16].

2.2. Statistics of the random fluctuations. The most convenient choice for the analysis would be having a Gaussian μ . However, since Gaussian processes are unbounded, this choice is inconsistent with equation (1.1), whose right hand side must be positive. We assume instead that μ is defined by a smooth and bounded function of a Gaussian process, which averages to zero so that $\mathbb{E}[\mu] = 0$. This gives a consistent random perturbation model, while keeping the analysis simple enough.

The covariance of μ is the inverse Fourier transform of the power spectrum (1.2)

$$\begin{aligned}
\text{Cov}_\mu(\mathbf{X}, z) &= \mathbb{E}[\mu(\mathbf{X}', z')\mu(\mathbf{X}' + \mathbf{X}, z' + z)] = \frac{1}{(2\pi)^3} \int_{\mathbb{R}^3} d\vec{\kappa} \cos[\vec{\kappa} \cdot (\mathbf{X}, z)] \mathbb{S}(\vec{\kappa}) \\
&= \frac{\chi_\alpha}{(2\pi)^3} \int_{L_o^{-1}}^{l_o^{-1}} d\kappa \kappa^2 \int_0^{2\pi} d\varphi \int_0^\pi d\vartheta \sin \vartheta \kappa^{-2-\alpha} \cos[\kappa|(\mathbf{X}, z)| \cos \vartheta] \\
&= \frac{\chi_\alpha}{2\pi^2} \int_{L_o^{-1}}^{l_o^{-1}} d\kappa \kappa^{-\alpha} \text{sinc}[\kappa|(\mathbf{X}, z)|] \\
&= \frac{\chi_\alpha |(\mathbf{X}, z)|^{\alpha-1}}{2\pi^2} \int_{|(\mathbf{X}, z)|/L_o}^{l_o^{-1}|(\mathbf{X}, z)|/L_o} ds s^{-\alpha} \text{sinc}(s). \tag{2.12}
\end{aligned}$$

Here we introduced the spherical coordinates $\vec{\kappa} \mapsto (\kappa, \varphi, \vartheta)$, with $\kappa = |\vec{\kappa}|$ and angles $\varphi \in (0, 2\pi)$ and $\vartheta \in (0, \pi)$. We also changed the variable of integration to $s = \kappa|(\mathbf{X}, z)|$. The variance of μ is obtained from equation (2.12) evaluated at the origin,

$$\text{Var}_\mu = \mathbb{E}[\mu^2(\mathbf{X}, z)] = \frac{\chi_\alpha}{2\pi^2} \int_{L_o^{-1}}^{l_o^{-1}} d\kappa \kappa^{-\alpha} = \frac{\chi_\alpha}{2\pi^2} \left(\frac{L_o^{\alpha-1} - l_o^{\alpha-1}}{\alpha - 1} \right). \tag{2.13}$$

We distinguish the following two cases in the paper. The first one is used in the analysis in sections 3 and 4, while the other one is used for comparison with the optics literature in section 5.

• **$\alpha \in (0, 1)$ and infinite outer scale:** When the initial radius r_s of the beam satisfies the order relation $l_o \lesssim r_s \ll L_o$, we can carry out the analysis in the limit $L_o \rightarrow \infty$, while keeping l_o finite. The variance (2.13) is finite in this limit

$$\text{Var}_\mu = \frac{\chi_\alpha}{2\pi^2(1-\alpha)l_o^{1-\alpha}}, \quad \alpha \in (0, 1), \quad L_o \rightarrow \infty, \tag{2.14}$$

but the covariance (2.12) is not integrable. In particular, we obtain from (2.12) that

$$\text{Cov}_\mu(\mathbf{0}, z) = \frac{\chi_\alpha |z|^{\alpha-1}}{2\pi^2} \int_0^{|z|/l_o} ds s^{-\alpha} \text{sinc}(s) \sim \frac{C_\alpha}{2\pi^2} |z|^{\alpha-1}, \quad \text{as } |z| \rightarrow \infty, \tag{2.15}$$

where the symbol “ \sim ” denotes an asymptotic expansion and, according to [21, Formula 3.761.4],

$$C_\alpha = \chi_\alpha \int_0^\infty ds s^{-\alpha} \text{sinc}(s) = \frac{\pi \chi_\alpha}{2 \cos(\alpha\pi/2) \Gamma(1+\alpha)}. \tag{2.16}$$

The slow decay at $|z| \rightarrow \infty$ in (2.15) implies that Cov_μ is non-integrable and we say that the process μ has long-range correlations.

• **$\alpha \in (0, 1) \cup (1, 2)$ and a finite outer scale:** When the beam has a larger radius, meaning that $l_o \lesssim r_s \lesssim L_o$, it experiences the random fluctuations in a different way than above, even for $\alpha < 1$. Indeed, integration by parts gives the estimate

$$\begin{aligned}
\left| \int_{|z|/L_o}^\infty ds s^{-\alpha} \text{sinc}(s) \right| &= \left| \left(\frac{|z|}{L_o} \right)^{-\alpha-1} \cos\left(\frac{|z|}{L_o} \right) - (1+\alpha) \int_{|z|/L_o}^\infty ds s^{-\alpha-2} \cos(s) \right| \\
&\leq \left(\frac{|z|}{L_o} \right)^{-\alpha-1} + (1+\alpha) \int_{|z|/L_o}^\infty ds s^{-\alpha-2} = 2 \left(\frac{|z|}{L_o} \right)^{-\alpha-1},
\end{aligned}$$

and substituting into (2.12) evaluated at $(\mathbf{X}, z) = (\mathbf{0}, z)$ we get

$$\text{Cov}_\mu(\mathbf{0}, z) \leq \frac{\chi_\alpha L_o^{\alpha+1}}{\pi^2} |z|^{-2}, \quad \text{as } |z| \rightarrow \infty. \quad (2.17)$$

The decay at $|z| \rightarrow \infty$ is now fast enough to make the covariance integrable and we say that the process μ is mixing.

Note from (2.13) that when $\alpha \in (1, 2)$, the variance of μ is finite only for a finite outer scale L_o , while the inner scale can be either finite or tend to 0. For the case $\alpha \in (0, 1)$ the variance blows up in the limit $l_o \rightarrow 0$, but it is finite for $L_o \rightarrow \infty$.

3. Asymptotic analysis for the long-range correlation case. We now describe the solution φ^ε of the paraxial equation (2.10-2.11) in the asymptotic limit $\varepsilon \rightarrow 0$, for $\alpha \in (0, 1)$ and an infinite outer scale. This case is interesting because the process μ has long-range correlations and there are two range scales that describe the randomization of φ^ε . We show in subsection 3.1 that φ^ε develops a significant random phase at a short, ε dependent range scale. Thus, in order to analyze it at longer range, we need to remove this random phase i.e., observe φ^ε in a random travel time frame, as explained in section 3.2.

3.1. Random central axis travel time analysis. We obtain from equations (1.1) and (2.6) that the random velocity along the axis of the beam is given by

$$\frac{c_o}{c^\varepsilon(\mathbf{0}, z)} = \sqrt{1 + \mu^\varepsilon(\bar{\mathbf{x}})} \sim 1 + \frac{\varepsilon^3}{2} \mu\left(\mathbf{0}, \frac{z}{\varepsilon^2}\right), \quad \text{as } \varepsilon \rightarrow 0, \quad (3.1)$$

so the central axis travel time is

$$\int_0^z \frac{dz'}{c^\varepsilon(\mathbf{0}, z')} \sim \frac{z}{c_o} + \frac{\varepsilon^4 \mathcal{Z}^\varepsilon(z)}{c_o}, \quad \mathcal{Z}^\varepsilon(z) = \frac{1}{2\varepsilon} \int_0^z dz' \mu\left(\mathbf{0}, \frac{z'}{\varepsilon^2}\right), \quad (3.2)$$

and has random fluctuations modeled by \mathcal{Z}^ε . Due to the high frequency $\omega = \frac{\Omega}{\varepsilon^4}$, these fluctuations have a significant effect on the phase of the wave field

$$\frac{\Omega}{\varepsilon^4} \int_0^z \frac{dz'}{c^\varepsilon(\mathbf{0}, z')} \sim \frac{k(\Omega)z}{\varepsilon^4} + k(\Omega)\mathcal{Z}^\varepsilon(z), \quad (3.3)$$

and the next proposition describes the asymptotics of \mathcal{Z}^ε , as $\varepsilon \rightarrow 0$.

PROPOSITION 3.1. *The random process \mathcal{Z}^ε defined in (3.2) satisfies*

$$\mathcal{Z}^\varepsilon\left(\varepsilon^{2\alpha/(1+\alpha)}z\right) \rightarrow C_H W^H(z), \quad \text{as } \varepsilon \rightarrow 0, \quad (3.4)$$

where the convergence is in distribution, $W^H(z)$ is a fractional Brownian motion with Hurst index $H = (1 + \alpha)/2$, and $C_H = \frac{1}{2\pi} \sqrt{\frac{C_\alpha}{\alpha(\alpha+1)}}$, with C_α given in (2.16). At $O(1)$ range the process \mathcal{Z}^ε satisfies

$$\varepsilon^\alpha \mathcal{Z}^\varepsilon(z) \rightarrow C_H W^H(z), \quad \text{as } \varepsilon \rightarrow 0, \quad (3.5)$$

where the convergence is in distribution and the limit is as in (3.4).

Proof. The convergence is proved in [29] for a Gaussian μ . The result extends to a process μ given by a smooth and bounded function of a Gaussian process as shown in [30] where the precise conditions on the function are given. \square

We recall from [28] that the fractional Brownian motion W^H is a Gaussian process, with stationary increments, satisfying

$$\mathbb{E}[W^H(z)] = 0, \quad \mathbb{E}[W^H(z)W^H(z')] = \frac{1}{2}[z^{2H} + (z')^{2H} + |z - z'|^{2H}]. \quad (3.6)$$

The proposition says that:

1. The process $\mathcal{Z}^\varepsilon(z)$ and therefore the phase (3.3) are randomized i.e., have significant random fluctuations, on a short $O(\varepsilon^{2\alpha/(1+\alpha)})$ range scale. In the physical variables (2.5), this corresponds to a propagation distance which is such that $k(\omega_0^\varepsilon)^2 \mathbb{E}[(\varepsilon^4 \mathcal{Z}^\varepsilon(z))^2] \sim 1$, that is to say, $z \sim [k(\omega_0^\varepsilon)^2 \chi_\alpha^\varepsilon]^{-1/(1+\alpha)}$.
2. Even though μ is not a Gaussian process, the phase fluctuations are Gaussian.
3. The random fluctuations of the phase are huge i.e., $O(\varepsilon^{-\alpha})$ at $O(1)$ range and must be removed in order to characterize the $\varepsilon \rightarrow 0$ limit of φ^ε .

3.2. Wave in the random travel time frame. After removing the random phase, which is equivalent to observing the wave in the central axis random time frame $\mathcal{Z}^\varepsilon/c_o$, we get that

$$\psi^\varepsilon(\Omega, \mathbf{X}, z) = \varphi^\varepsilon(\Omega, \mathbf{X}, z) \exp[-ik(\Omega)\mathcal{Z}^\varepsilon(z)], \quad (3.7)$$

satisfies the paraxial equation

$$\left[2ik(\Omega)\partial_z + \Delta_{\mathbf{X}} + \frac{k^2(\Omega)}{\varepsilon} \nu\left(\mathbf{X}, \frac{z}{\varepsilon^2}\right) \right] \psi^\varepsilon(\Omega, \mathbf{X}, z) = 0, \quad z > 0, \quad (3.8)$$

$$\psi^\varepsilon(\Omega, \mathbf{X}, z=0) = \hat{F}(\Omega, \mathbf{X}), \quad (3.9)$$

with the random potential

$$\nu(\mathbf{X}, z) = \mu(\mathbf{X}, z) - \mu(\mathbf{0}, z). \quad (3.10)$$

The process ν is stationary in z , but not in \mathbf{X} , and we explain next that its covariance is integrable in z . Indeed,

$$\begin{aligned} \text{Cov}_\nu(\mathbf{X}, \mathbf{X}', z - z') &= \mathbb{E}[\nu(\mathbf{X}, z)\nu(\mathbf{X}', z')] = \text{Cov}_\mu(\mathbf{X} - \mathbf{X}', z - z') \\ &\quad + \text{Cov}_\mu(\mathbf{0}, z - z') - \text{Cov}_\mu(\mathbf{X}', z - z') - \text{Cov}_\mu(\mathbf{X}, z - z'), \end{aligned} \quad (3.11)$$

and using equation (2.12) we get for $\mathbf{X} = \mathbf{X}'$:

$$\begin{aligned} \text{Cov}_\nu(\mathbf{X}, \mathbf{X}, z) &= \frac{\chi_\alpha |z|^{\alpha-1}}{\pi^2} \left[\int_0^{|z|/l_o} du u^{-\alpha} \text{sinc}(u) \right. \\ &\quad \left. - \left(1 + \frac{|\mathbf{X}|^2}{z^2}\right)^{(\alpha-1)/2} \int_0^{|z|/l_o \sqrt{1+|\mathbf{X}|^2/z^2}} du u^{-\alpha} \text{sinc}(u) \right]. \end{aligned} \quad (3.12)$$

We are interested in the decay of this expression at $|z| \rightarrow \infty$, which can be seen from the asymptotic expansion

$$\begin{aligned} \text{Cov}_\nu(\mathbf{X}, \mathbf{X}, z) &\sim \frac{C_\alpha}{\pi^2} |z|^{\alpha-1} \left[1 - \left(1 + \frac{|\mathbf{X}|^2}{z^2}\right)^{(\alpha-1)/2} \right] \\ &\sim \frac{C_\alpha(1-\alpha)|\mathbf{X}|^2}{2\pi^2} |z|^{\alpha-3}, \quad \text{as } |z| \rightarrow \infty, \end{aligned} \quad (3.13)$$

with constant C_α given by (2.16). Since $\alpha \in (0, 1)$, the decay in $|z|$ is fast enough to make the covariance integrable, and we say that the process ν is mixing.

PROPOSITION 3.2. *The solution ψ^ε of (3.8-3.9) converges in distribution, in the space $C([0, +\infty), L^2(\mathbb{R} \times \mathbb{R}^2, \mathbb{C}))$ of continuous functions of $z \in [0, \infty)$ that are square integrable in (Ω, \mathbf{X}) , to the solution of the Itô-Schrödinger equation*

$$d\psi(\Omega, \mathbf{X}, z) = \frac{i}{2k(\Omega)} \Delta_{\mathbf{X}} \psi(\Omega, \mathbf{X}, z) dz + \frac{ik(\Omega)}{2} \psi(\Omega, \mathbf{X}, z) \circ dW(\mathbf{X}, z), \quad (3.14)$$

with initial condition

$$\psi(\Omega, \mathbf{X}, z = 0) = \hat{F}(\Omega, \mathbf{X}). \quad (3.15)$$

The symbol “ \circ ” denotes the Stratonovich integral and $W(\mathbf{X}, z)$ is a centered Brownian field. It satisfies $\mathbb{E}[W(\mathbf{X}, z)W(\mathbf{X}', z')] = \gamma(\mathbf{X}, \mathbf{X}') \min(z, z')$, with

$$\gamma(\mathbf{X}, \mathbf{X}') = \frac{\chi_\alpha}{2\pi} \int_0^{l_0^{-1}} d\kappa [J_0(\kappa|\mathbf{X} - \mathbf{X}'|) + 1 - J_0(\kappa|\mathbf{X}|) - J_0(\kappa|\mathbf{X}'|)] \kappa^{-1-\alpha}, \quad (3.16)$$

where J_0 is the Bessel function of the first kind and of order 0.

Proof. This theorem was proved for a fixed frequency in [14]: For any $\Omega \neq 0$, the solution $(z, \mathbf{X}) \mapsto \psi^\varepsilon(\Omega, \mathbf{X}, z)$ of (3.8) converges in distribution, in the space $D([0, +\infty), L^2(\mathbb{R}^2, \mathbb{C}))$, to the solution $(z, \mathbf{X}) \mapsto \psi(\Omega, \mathbf{X}, z)$ of (3.14). Here D is the space of càdlàg functions. The proof can be extended to the multi-frequency case as follows: for any set of non-zero frequencies $(\Omega_j)_{j=1}^n$, the random process $(z, \mathbf{X}) \mapsto (\psi^\varepsilon(\Omega_j, \mathbf{X}, z))_{j=1}^n$ converges in distribution in $D([0, +\infty), L^2(\mathbb{R}^2, \mathbb{C}^n))$ to the process $(z, \mathbf{X}) \mapsto (\psi(\Omega_j, \mathbf{X}, z))_{j=1}^n$.

The tightness of ψ^ε in $D([0, +\infty), L_w^2(\mathbb{R} \times \mathbb{R}^2, \mathbb{C}))$ (with L_w^2 equipped with the weak topology) can be established as in [14, Section 3.1] by using the tightness criterion [25, Chap. 3, Theorem 4]. This proves the convergence of ψ^ε to ψ in the space $D([0, +\infty), L_w^2(\mathbb{R} \times \mathbb{R}^2, \mathbb{C}))$. Since both the original and limit processes preserve the L^2 -norm of the initial data, the process converges in $D([0, +\infty), L^2(\mathbb{R} \times \mathbb{R}^2, \mathbb{C}))$. Furthermore, since both the original and limit processes are continuous, the convergence actually holds in $C([0, +\infty), L^2(\mathbb{R} \times \mathbb{R}^2, \mathbb{C}))$. \square

4. Application of the asymptotic analysis. We now use the asymptotic results stated in Propositions 3.1 and 3.2 to analyze the coherent wave (subsection 4.1) and the spatial and frequency covariance of φ^ε (subsections 4.2–4.3) in the limit $\varepsilon \rightarrow 0$. We also characterize in subsection 4.4 the deformation of the pulse emitted by the source, induced by scattering in the random medium.

4.1. The coherent wave. Scattering causes a loss of coherence of the wave field, which manifests as an exponential decay of the mean wave (aka coherent wave) $\mathbb{E}[\varphi^\varepsilon]$ with respect to the range z . The length scale of decay, called the scattering mean free path, gives the range limit at which conventional methods* used for imaging and free space communication are useful in random media.

The leading factor in the loss of coherence of φ^ε is the random phase $k\mathcal{Z}^\varepsilon$, which becomes significant at $O(\varepsilon^{2\alpha/(1+\alpha)})$ range. Indeed, Propositions 3.1 and 3.2 give that

$$\mathbb{E}\left[\exp(ik(\Omega)\mathcal{Z}^\varepsilon(\varepsilon^{2\alpha/(1+\alpha)}z))\right] \xrightarrow{\varepsilon \rightarrow 0} \exp\left[-\frac{C_H^2 k^2(\Omega)z^{2H}}{2}\right] \quad (4.1)$$

*Conventional methods are based on the assumption that the medium through which the waves propagate is homogeneous or more generally, known and non-scattering.

and

$$\mathbb{E}[\varphi^\varepsilon(\Omega, \mathbf{X}, \varepsilon^{2\alpha/(1+\alpha)}z)] \xrightarrow{\varepsilon \rightarrow 0} \widehat{F}(\Omega, \mathbf{X}) \exp\left[-\frac{C_H^2 k^2(\Omega) z^{2H}}{2}\right], \quad (4.2)$$

so the scattering mean free path has the asymptotic expansion

$$\mathcal{L}_{\varphi^\varepsilon}(\Omega) \sim \varepsilon^{2\alpha/(1+\alpha)} [C_H k(\Omega)]^{-1/H}. \quad (4.3)$$

However, the wave ψ^ε defined in (3.7) by removing the large random phase $k\mathcal{Z}^\varepsilon$ from φ^ε , maintains its coherence up to a much longer, $O(1)$ range. Proposition 3.2 gives that

$$\mathbb{E}[\psi^\varepsilon(\Omega, \mathbf{X}, z)] \xrightarrow{\varepsilon \rightarrow 0} M_1(\Omega, \mathbf{X}, z), \quad (4.4)$$

where M_1 solves the evolution equation

$$\partial_z M_1(\Omega, \mathbf{X}, z) = \frac{i}{2k(\Omega)} \Delta_{\mathbf{X}} M_1(\Omega, \mathbf{X}, z) - \frac{k^2(\Omega)}{4} \Theta(\mathbf{X}) M_1(\Omega, \mathbf{X}, z), \quad (4.5)$$

obtained by taking the expectation in (3.14), with initial condition derived from (3.15)

$$M_1(\Omega, \mathbf{X}, z=0) = \widehat{F}(\Omega, \mathbf{X}), \quad (4.6)$$

and with damping coefficient

$$\begin{aligned} \Theta(\mathbf{X}) &= \frac{\gamma(\mathbf{X}, \mathbf{X})}{2} = \frac{\chi_\alpha}{2\pi} \int_0^{l_0^{-1}} d\kappa [1 - J_0(\kappa|\mathbf{X}|)] \kappa^{-1-\alpha} \\ &= \frac{\chi_\alpha |\mathbf{X}|^\alpha}{2\pi} \int_0^{|\mathbf{X}|/l_0} ds [1 - J_0(s)] s^{-1-\alpha}. \end{aligned} \quad (4.7)$$

The damping models the loss of coherence of ψ^ε . It is weaker at the axis of the beam and it increases away from it. In fact, at $|\mathbf{X}|/l_0 \rightarrow \infty$ we get the asymptotic expansion

$$\Theta(\mathbf{X}) \sim d_\alpha |\mathbf{X}|^\alpha, \quad d_\alpha = \frac{\chi_\alpha}{2\pi} \int_0^\infty ds [1 - J_0(s)] s^{-1-\alpha} = \frac{\chi_\alpha}{2^{1+\alpha}\pi} \frac{\Gamma(1-\alpha/2)}{\alpha\Gamma(1+\alpha/2)}. \quad (4.8)$$

4.2. Spatial covariance. Although the wave loses its coherence (the mean wave decays with the propagation distance), wave energy is not lost but converted into incoherent, zero-mean fluctuations. These incoherent waves can be characterized by the second-order moments of the wave field, that we analyze in this subsection and the next ones. For imaging purposes, it is possible to extract information from the observation of the incoherent waves and their correlation properties in space and frequency. An example of exploiting such knowledge is the coherent interferometric (CINT) methodology for robust imaging in random media [5, 6, 8].

There are two intrinsic scales that capture the decorrelation properties of the wave field: the ‘‘decoherence length’’, which is the length scale of decay of the covariance of φ^ε over cross-range offsets and the ‘‘decoherence frequency’’, which is the frequency scale of decay of the covariance over frequency offsets. In this subsection we study the spatial covariance i.e., fix the frequency at Ω , and estimate the decoherence length. We note from definition (3.7) that the phase $k\mathcal{Z}^\varepsilon$ plays no role in the spatial covariance,

$$\mathbb{E}[\varphi^\varepsilon(\Omega, \mathbf{X}_1, z) \overline{\varphi^\varepsilon(\Omega, \mathbf{X}_2, z)}] = \mathbb{E}[\psi^\varepsilon(\Omega, \mathbf{X}_1, z) \overline{\psi^\varepsilon(\Omega, \mathbf{X}_2, z)}] \xrightarrow{\varepsilon \rightarrow 0} \mathcal{C}_\Omega(\mathbf{X}_1, \mathbf{X}_2, z).$$

Here the bar stands for the complex conjugate, the notation \mathcal{C}_Ω emphasizes that the frequency is fixed at Ω , and the $\varepsilon \rightarrow 0$ limit

$$\mathcal{C}_\Omega(\mathbf{X}_1, \mathbf{X}_2, z) = \mathbb{E}[\psi(\Omega, \mathbf{X}_1, z) \overline{\psi(\Omega, \mathbf{X}_2, z)}] \quad (4.9)$$

is obtained from the Itô-Schrödinger equation in Proposition 3.2. Using the identity

$$\gamma(\mathbf{X}_1, \mathbf{X}_2) - \Theta(\mathbf{X}_1) - \Theta(\mathbf{X}_2) = -\Theta(\mathbf{X}_1 - \mathbf{X}_2),$$

deduced from definitions (3.16) and (4.7), we get the evolution equation

$$\partial_z \mathcal{C}_\Omega(\mathbf{X}_1, \mathbf{X}_2, z) = \left[\frac{i}{2k(\Omega)} (\Delta_{\mathbf{X}_1} - \Delta_{\mathbf{X}_2}) - \frac{k^2(\Omega)}{4} \Theta(\mathbf{X}_1 - \mathbf{X}_2) \right] \mathcal{C}_\Omega(\mathbf{X}_1, \mathbf{X}_2, z), \quad (4.10)$$

for $z > 0$, with initial condition

$$\mathcal{C}_\Omega(\mathbf{X}_1, \mathbf{X}_2, z=0) = \widehat{F}(\Omega, \mathbf{X}_1) \overline{\widehat{F}(\Omega, \mathbf{X}_2)}. \quad (4.11)$$

We can solve equation (4.10) explicitly, by changing coordinates

$$(\mathbf{X}_1, \mathbf{X}_2) \mapsto (\mathbf{X}, \mathbf{Y}), \quad \mathbf{X} = \frac{1}{2}(\mathbf{X}_1 + \mathbf{X}_2), \quad \mathbf{Y} = \mathbf{X}_1 - \mathbf{X}_2, \quad (4.12)$$

and then taking the Fourier transform with respect to the offset vector \mathbf{Y} , which defines the mean Wigner transform

$$\mathcal{W}_\Omega(\mathbf{X}, \boldsymbol{\kappa}, z) = \int_{\mathbb{R}^2} d\mathbf{Y} \mathcal{C}_\Omega\left(\mathbf{X} + \frac{\mathbf{Y}}{2}, \mathbf{X} - \frac{\mathbf{Y}}{2}, z\right) e^{-i\boldsymbol{\kappa} \cdot \mathbf{Y}}. \quad (4.13)$$

This transform is important by itself, as it tells us how the energy at \mathbf{X} is distributed over the directions i.e., along $\boldsymbol{\kappa}$. It plays a key role in the analysis of imaging and time reversal methods in random media [6, 9, 31]. The calculation of \mathcal{W}_Ω is given in Appendix A and the result is stated in the following proposition:

PROPOSITION 4.1. *The mean Wigner transform is given by*

$$\begin{aligned} \mathcal{W}_\Omega(\mathbf{X}, \boldsymbol{\kappa}, z) &= \frac{1}{(2\pi)^2} \int_{\mathbb{R}^2} d\mathbf{q} \int_{\mathbb{R}^2} d\mathbf{Y} \exp \left[i\mathbf{q} \cdot \left(\mathbf{X} - \boldsymbol{\kappa} \frac{z}{k(\Omega)} \right) - i\boldsymbol{\kappa} \cdot \mathbf{Y} \right] \widehat{\mathcal{W}}_{\Omega,0}(\mathbf{q}, \mathbf{Y}) \\ &\quad \times \exp \left[-\frac{k^2(\Omega)}{4} \int_0^z dz' \Theta\left(\mathbf{Y} + \frac{\mathbf{q}z'}{k(\Omega)}\right) \right], \end{aligned} \quad (4.14)$$

with

$$\widehat{\mathcal{W}}_{\Omega,0}(\mathbf{q}, \mathbf{Y}) = \int_{\mathbb{R}^2} d\mathbf{X} \widehat{F}\left(\Omega, \mathbf{X} + \frac{\mathbf{Y}}{2}\right) \overline{\widehat{F}\left(\Omega, \mathbf{X} - \frac{\mathbf{Y}}{2}\right)} e^{-i\mathbf{q} \cdot \mathbf{X}}. \quad (4.15)$$

The spatial covariance is obtained from the expression (4.14) using the inverse Fourier transform

$$\begin{aligned} \mathcal{C}_\Omega\left(\mathbf{X} + \frac{\mathbf{Y}}{2}, \mathbf{X} - \frac{\mathbf{Y}}{2}, z\right) &= \frac{1}{(2\pi)^2} \int_{\mathbb{R}^2} d\boldsymbol{\kappa} \mathcal{W}_\Omega(\mathbf{X}, \boldsymbol{\kappa}, z) e^{i\boldsymbol{\kappa} \cdot \mathbf{Y}} \\ &= \frac{1}{(2\pi)^2} \int_{\mathbb{R}^2} d\mathbf{q} \widehat{\mathcal{W}}_{\Omega,0}\left(\mathbf{q}, \mathbf{Y} - \frac{\mathbf{q}z}{k(\Omega)}\right) e^{i\mathbf{q} \cdot \mathbf{X}} \\ &\quad \times \exp \left[-\frac{k^2(\Omega)}{4} \int_0^z dz' \Theta\left(\mathbf{Y} - \frac{\mathbf{q}(z-z')}{k(\Omega)}\right) \right], \end{aligned} \quad (4.16)$$

and we study it next using the asymptotic expansion (4.8) of Θ , which holds when its argument is much larger than l_o . Note that the coefficient d_α in this expansion quantifies the strength of the fluctuations in the random medium.

We have already assumed a large outer scale L_o . We now consider, in addition, a strong fluctuation and small inner scale regime, in the sense

$$l_o \ll \frac{1}{Q(z)} \ll r_s \ll R(z), \quad (4.17)$$

where we recall that r_s is the initial radius of the beam. There are two new scales in equation (4.17): the range dependent beam radius

$$R(z) = \left[\frac{d_\alpha k^{2-\alpha}(\Omega) z^{\alpha+1}}{\alpha+1} \right]^{1/\alpha}, \quad (4.18)$$

which quantifies the spatial support of the mean intensity (subsection 4.2.1), and the range dependent wave vector radius

$$Q(z) = [d_\alpha k^2(\Omega) z]^{1/\alpha}, \quad (4.19)$$

which quantifies the wave vector support of the mean spectrum (subsection 4.2.2).

4.2.1. The mean intensity. The mean intensity $\mathbb{E} [|\psi(\Omega, \mathbf{X}, z)|^2]$ is equal to $\mathcal{C}_\Omega(\mathbf{X}, \mathbf{X}, z)$. From Proposition 4.1 we obtain the following result.

PROPOSITION 4.2. *In the regime (4.17), the mean intensity has the form*

$$\mathbb{E} [|\psi(\Omega, \mathbf{X}, z)|^2] \simeq \frac{\widehat{\mathcal{W}}_{\Omega,0}(\mathbf{0}, \mathbf{0})}{R^2(z)} \Psi_\alpha\left(\frac{\mathbf{X}}{R(z)}\right), \quad (4.20)$$

with $\widehat{\mathcal{W}}_{\Omega,0}$ given by (4.15) and

$$\Psi_\alpha(\boldsymbol{\xi}) = \frac{1}{(2\pi)^2} \int_{\mathbb{R}^2} d\boldsymbol{\eta} e^{i\boldsymbol{\eta} \cdot \boldsymbol{\xi} - \frac{|\boldsymbol{\eta}|^\alpha}{4}} = \frac{1}{2\pi} \int_0^\infty d\eta \eta J_0(|\boldsymbol{\xi}|\eta) e^{-\frac{\eta^\alpha}{4}}. \quad (4.21)$$

Proof. Setting $\mathbf{Y} = \mathbf{0}$ in (4.16) and using the asymptotic expansion (4.8) we obtain the following expression of the mean intensity

$$\begin{aligned} \mathbb{E} [|\psi(\Omega, \mathbf{X}, z)|^2] &= \frac{1}{(2\pi)^2} \int_{\mathbb{R}^2} d\mathbf{q} \widehat{\mathcal{W}}_{\Omega,0}\left(\mathbf{q}, -\frac{\mathbf{q}z}{k(\Omega)}\right) \exp\left[i\mathbf{q} \cdot \mathbf{X} - \frac{R^\alpha(z)|\mathbf{q}|^\alpha}{4}\right] \\ &= \frac{1}{(2\pi)^2 R^2(z)} \int_{\mathbb{R}^2} d\boldsymbol{\eta} \widehat{\mathcal{W}}_{\Omega,0}\left(\frac{\boldsymbol{\eta}}{R(z)}, -\frac{\boldsymbol{\eta}z}{k(\Omega)R(z)}\right) \exp\left[i\frac{\boldsymbol{\eta} \cdot \mathbf{X}}{R(z)} - \frac{|\boldsymbol{\eta}|^\alpha}{4}\right], \end{aligned}$$

where we let $\mathbf{q} = \boldsymbol{\eta}/R$, with R defined in (4.18). Due to the exponential, only $|\boldsymbol{\eta}| = O(1)$ contributes to the integral, so the arguments of $\widehat{\mathcal{W}}_{\Omega,0}$ satisfy

$$\frac{|\boldsymbol{\eta}|}{R(z)} = O(R^{-1}(z)) \ll r_s^{-1}, \quad \frac{|\boldsymbol{\eta}|z}{k(\Omega)R(z)} = O\left(\frac{z}{k(\Omega)R(z)}\right) \ll r_s. \quad (4.22)$$

Here we used the assumption (4.17) and the second inequality is because by definitions (4.18-4.19) we have

$$\frac{z}{k(\Omega)R(z)} = \frac{(\alpha+1)^{1/\alpha}}{[d_\alpha k^2(\Omega)z]^{1/\alpha}} = \frac{(\alpha+1)^{1/\alpha}}{Q(z)} \ll r_s.$$

We infer from definition (4.15) of $\widehat{\mathcal{W}}_{\Omega,0}$ that its support in the first argument is at wave vectors with $O(r_s^{-1})$ norm and the support in the second argument is at cross-range vectors of $O(r_s)$ norm. Thus, due to the inequalities (4.22), we can approximate the mean intensity by (4.20). \square

We plot the function Ψ_α in section 5. It peaks at the origin and it is negligible outside a disk of $O(1)$ radius. It is smooth at $\mathbf{0}$ and can be expanded as

$$\Psi_\alpha(\boldsymbol{\xi}) = \Psi_\alpha(\mathbf{0})[1 - q_\alpha|\boldsymbol{\xi}|^2 + o(|\boldsymbol{\xi}|^2)], \quad (4.23)$$

where

$$\Psi_\alpha(\mathbf{0}) = \frac{2^{4/\alpha}\Gamma(2/\alpha)}{2\pi\alpha}, \quad q_\alpha = 2^{4/\alpha-2}\frac{\Gamma(4/\alpha)}{\Gamma(2/\alpha)}. \quad (4.24)$$

Therefore, the scale $R(z)$ quantifies the support of the mean intensity, and we call it the ‘‘beam radius’’ at range z . If there were no random medium, beam broadening would be entirely due to diffraction. Here the broadening is caused by scattering in the random medium and it is significant, because $R(z)$ is much larger than the initial radius r_s of the beam, per equation (4.17) and with a growth rate in z that is higher than in the homogeneous medium.

4.2.2. The mean spectrum. Using the Fourier transform

$$\widehat{\psi}(\Omega, \boldsymbol{\kappa}, z) = \int_{\mathbb{R}^2} d\mathbf{X} \psi(\Omega, \mathbf{X}, z) e^{-i\boldsymbol{\kappa}\cdot\mathbf{X}},$$

the change of coordinates (4.12) and the definition (4.13) of the Wigner transform, we can calculate the mean spectrum as follows

$$\begin{aligned} \mathbb{E}[|\widehat{\psi}(\Omega, \boldsymbol{\kappa}, z)|^2] &= \int_{\mathbb{R}^2} d\mathbf{X}_1 \int_{\mathbb{R}^2} d\mathbf{X}_2 \mathbb{E}[\psi(\Omega, \mathbf{X}_1, z) \overline{\psi(\Omega, \mathbf{X}_2, z)}] e^{i\boldsymbol{\kappa}\cdot(\mathbf{X}_2 - \mathbf{X}_1)} \\ &= \int_{\mathbb{R}^2} d\mathbf{X} \int_{\mathbb{R}^2} d\mathbf{Y} \mathcal{C}_\Omega\left(\mathbf{X} + \frac{\mathbf{Y}}{2}, \mathbf{X} - \frac{\mathbf{Y}}{2}, z\right) e^{-i\boldsymbol{\kappa}\cdot\mathbf{Y}} \\ &= \int_{\mathbb{R}^2} d\mathbf{X} \mathcal{W}_\Omega(\mathbf{X}, \boldsymbol{\kappa}, z), \end{aligned}$$

with right-hand side given in Proposition 4.1. We then obtain the following result.

PROPOSITION 4.3. *In the regime (4.17), the mean spectrum is of the form*

$$\mathbb{E}[|\widehat{\psi}(\Omega, \boldsymbol{\kappa}, z)|^2] \simeq \frac{(2\pi)^2 \widehat{\mathcal{W}}_{\Omega,0}(\mathbf{0}, \mathbf{0})}{Q^2(z)} \Psi_\alpha\left(\frac{\boldsymbol{\kappa}}{Q(z)}\right), \quad (4.25)$$

with Ψ_α defined in (4.21).

Proof. Using the asymptotic expansion (4.8) of Θ and integrating over \mathbf{X} and \mathbf{q} we get

$$\begin{aligned} \mathbb{E}[|\widehat{\psi}(\Omega, \boldsymbol{\kappa}, z)|^2] &= \int_{\mathbb{R}^2} d\mathbf{Y} \widehat{\mathcal{W}}_{\Omega,0}(\mathbf{0}, \mathbf{Y}) \exp\left[-i\boldsymbol{\kappa}\cdot\mathbf{Y} - \frac{d_\alpha k^2(\Omega)z|\mathbf{Y}|^\alpha}{4}\right] \\ &= \frac{1}{Q^2(z)} \int_{\mathbb{R}^2} d\boldsymbol{\eta} \widehat{\mathcal{W}}_{\Omega,0}\left(\mathbf{0}, \frac{\boldsymbol{\eta}}{Q(z)}\right) \exp\left[-i\frac{\boldsymbol{\kappa}\cdot\boldsymbol{\eta}}{Q(z)} - \frac{|\boldsymbol{\eta}|^\alpha}{4}\right], \end{aligned}$$

with Q defined in (4.19). Arguing as before, since only $|\boldsymbol{\eta}| = O(1)$ contributes to the integral, due to the exponential, the argument of $\widehat{\mathcal{W}}_{\Omega,0}$ satisfies

$$\frac{|\boldsymbol{\eta}|}{Q(z)} = O(Q^{-1}(z)) \ll r_s,$$

and we can approximate the mean spectrum by (4.25). \square

This result shows that the scale Q quantifies the support of the spectrum, so we call it the ‘‘spectral radius’’ at range z . The initial spectral radius is $O(r_s^{-1})$, but due to scattering in the random medium it becomes significantly larger at $O(1)$ range, per equation (4.17). This goes hand in hand with the broadening of the beam described by equation (4.20).

4.2.3. The spatial covariance function. In the strong fluctuation regime (4.17) it is possible to express the covariance in terms of the beam radius R and wave vector radius Q as follows.

PROPOSITION 4.4. *In the regime (4.17), the covariance has the form*

$$\mathcal{C}_\Omega\left(\mathbf{X} + \frac{\mathbf{Y}}{2}, \mathbf{X} - \frac{\mathbf{Y}}{2}, z\right) \simeq \frac{\widehat{\mathcal{W}}_{\Omega,0}(\mathbf{0}, \mathbf{0})}{R^2(z)} \Phi_\alpha\left(\frac{\mathbf{X}}{R(z)}, \mathbf{Y}Q(z)\right), \quad (4.26)$$

with the function

$$\Phi_\alpha(\boldsymbol{\xi}, \boldsymbol{\zeta}) = \frac{1}{(2\pi)^2} \int_{\mathbb{R}^2} d\boldsymbol{\eta} \exp\left[i\boldsymbol{\eta} \cdot \boldsymbol{\xi} - \frac{(1+\alpha)}{4} \int_0^1 ds \left| \frac{\boldsymbol{\zeta}}{(1+\alpha)^{1/\alpha}} - \boldsymbol{\eta}s \right|^\alpha\right]. \quad (4.27)$$

Proof. Starting from equation (4.16), using the asymptotic expansion (4.8), changing variables as $s = (z - z')/z$ and $\boldsymbol{\eta} = R\boldsymbol{q}$, and using definitions (4.18) and (4.19) we get

$$\begin{aligned} \mathcal{C}_\Omega\left(\mathbf{X} + \frac{\mathbf{Y}}{2}, \mathbf{X} - \frac{\mathbf{Y}}{2}, z\right) &= \frac{1}{(2\pi)^2 R^2(z)} \int_{\mathbb{R}^2} d\boldsymbol{\eta} \widehat{\mathcal{W}}_{\Omega,0}\left(\frac{\boldsymbol{\eta}}{R(z)}, \mathbf{Y} - \frac{\boldsymbol{\eta}z}{k(\Omega)R(z)}\right) \\ &\quad \times \exp\left[i\frac{\boldsymbol{\eta} \cdot \mathbf{X}}{R(z)} - \frac{(1+\alpha)}{4} \int_0^1 ds \left| \frac{\mathbf{Y}Q(z)}{(1+\alpha)^{1/\alpha}} - \boldsymbol{\eta}s \right|^\alpha\right]. \end{aligned}$$

Again, we conclude that only $|\boldsymbol{\eta}| = O(1)$ contributes to the integral, due to the decaying exponential, so under the strong fluctuations assumption (4.17) we can make the approximation

$$\widehat{\mathcal{W}}_{\Omega,0}\left(\frac{\boldsymbol{\eta}}{R(z)}, \cdot\right) \approx \widehat{\mathcal{W}}_{\Omega,0}(\mathbf{0}, \cdot).$$

We also get from definitions (4.18-4.19) and the assumption (4.17) the following estimates

$$\frac{|\boldsymbol{\eta}|z}{k(\Omega)R(z)} = O(Q^{-1}(z)) \ll r_s, \quad |\mathbf{Y}| = O(Q^{-1}(z)) \ll r_s.$$

Here we used that $|\mathbf{Y}|Q = O(1)$ in order for the exponential to be large. Therefore, the covariance can be approximated by (4.26). \square

Note that $\Phi_\alpha(\boldsymbol{\xi}, \mathbf{0}) = \Psi_\alpha(\boldsymbol{\xi})$, with Ψ_α given in (4.21), and we also have

$$\int_{\mathbb{R}^2} d\boldsymbol{\xi} \int_{\mathbb{R}^2} d\boldsymbol{\zeta} \Phi_\alpha(\boldsymbol{\xi}, \boldsymbol{\zeta}) e^{-i\boldsymbol{\kappa} \cdot \boldsymbol{\zeta}} = (2\pi)^2 \Psi_\alpha(\boldsymbol{\kappa}). \quad (4.28)$$

Contrarily to the function $\boldsymbol{\xi} \mapsto \Phi_\alpha(\boldsymbol{\xi}, \mathbf{0})$ that is smooth at $\mathbf{0}$ by (4.23), the function $\boldsymbol{\zeta} \mapsto \Phi_\alpha(\mathbf{0}, \boldsymbol{\zeta})$ has a cusp at $\mathbf{0}$ (see Appendix B):

$$\Phi_\alpha(\mathbf{0}, \boldsymbol{\zeta}) = \Phi_\alpha(\mathbf{0}, \mathbf{0}) \left(1 - r_\alpha |\boldsymbol{\zeta}|^{\alpha+1} + o(|\boldsymbol{\zeta}|^{\alpha+1}) \right), \quad (4.29)$$

where r_α is given by

$$r_\alpha = \frac{\alpha}{2^{2+2/\alpha}(1+\alpha)^{1/\alpha+2}} \frac{\Gamma(1/\alpha)\Gamma(1/2-\alpha/2)\Gamma(1+\alpha/2)}{\Gamma(2/\alpha)\Gamma(1/2+\alpha/2)\Gamma(1-\alpha/2)}. \quad (4.30)$$

This implies that the covariance (4.26) has a cusp at $\mathbf{Y} = \mathbf{0}$.

We plot the marginals $\boldsymbol{\xi} \mapsto \Phi_\alpha(\boldsymbol{\xi}, \mathbf{0})$ and $\boldsymbol{\zeta} \mapsto \Phi_\alpha(\mathbf{0}, \boldsymbol{\zeta})$ in section 5. They peak at the origin and are negligible outside a disk with $O(1)$ radius. We conclude therefore, from (4.26), that Q^{-1} quantifies the length scale of decorrelation over the spatial offsets \mathbf{Y} at range z , so we can refer to it as the ‘‘decoherence length’’

$$\mathfrak{X}(z) = Q^{-1}(z) = O\left(\left(d_\alpha z\right)^{-1/\alpha} k^{-2/\alpha}(\Omega)\right). \quad (4.31)$$

This is proportional to the wavelength raised to the power $2/\alpha$, and it decreases with the range z and with the strength of the random medium, quantified by d_α .

4.3. The frequency covariance function. The leading factor in the frequency decorrelation of φ^ε at $O(1)$ range is the random phase $k(\Omega)\mathcal{Z}^\varepsilon$. Indeed, we obtain from Propositions 3.1–3.2 that this phase gives a significant contribution to the covariance for $O(\varepsilon^\alpha)$ frequency offsets,

$$\begin{aligned} \mathbb{E} \left[\varphi^\varepsilon \left(\Omega + \frac{\varepsilon^\alpha \tilde{\Omega}}{2}, \mathbf{X} + \frac{\mathbf{Y}}{2}, z \right) \overline{\varphi^\varepsilon \left(\Omega - \frac{\varepsilon^\alpha \tilde{\Omega}}{2}, \mathbf{X} - \frac{\mathbf{Y}}{2}, z \right)} \right] &\xrightarrow{\varepsilon \rightarrow 0} \exp \left[-\frac{\tilde{\Omega}^2 C_H^2 z^{2H}}{2c_o^2} \right] \\ &\times \mathcal{C}_\Omega \left(\mathbf{X} + \frac{\mathbf{Y}}{2}, \mathbf{X} - \frac{\mathbf{Y}}{2}, z \right). \end{aligned} \quad (4.32)$$

This contribution is described by the Gaussian in $\tilde{\Omega}$, whose standard deviation defines the decoherence frequency

$$\Omega_{\varphi^\varepsilon}(z) = \frac{c_o \varepsilon^\alpha}{C_H z^H}, \quad (4.33)$$

which decreases with the range z and with the strength of the random medium, quantified by d_α (see Proposition 3.1 for the definitions of H and C_H).

If the random phase is removed from φ^ε (which means, we observe the field around the central axis random arrival time), then the decoherence frequency is larger and it is described in the limit $\varepsilon \rightarrow 0$ by the decay in $|\Omega_1 - \Omega_2|$ of the covariance

$$\mathcal{C}(\Omega_1, \Omega_2, \mathbf{X}_1, \mathbf{X}_2, z) = \mathbb{E} \left[\psi(\Omega_1, \mathbf{X}_1, z) \overline{\psi(\Omega_2, \mathbf{X}_2, z)} \right]. \quad (4.34)$$

The evolution equation for this covariance is obtained from the Itô-Schrödinger equation in Proposition 3.2 and the definitions (3.16), (4.7),

$$\begin{aligned} \partial_z \mathcal{C}(\Omega_1, \Omega_2, \mathbf{X}_1, \mathbf{X}_2, z) &= \left\{ \frac{i}{2k_1} \Delta_{\mathbf{X}_1} - \frac{i}{2k_2} \Delta_{\mathbf{X}_2} - \left[\frac{k_1 k_2}{4} \Theta(\mathbf{X}_1 - \mathbf{X}_2) \right. \right. \\ &\left. \left. + \frac{k_1(k_1 - k_2)}{4} \Theta(\mathbf{X}_1) - \frac{k_2(k_1 - k_2)}{4} \Theta(\mathbf{X}_2) \right] \right\} \mathcal{C}(\Omega_1, \Omega_2, \mathbf{X}_1, \mathbf{X}_2, z), \end{aligned} \quad (4.35)$$

for $z > 0$, with initial condition

$$\mathcal{C}(\Omega_1, \Omega_2, \mathbf{X}_1, \mathbf{X}_2, z = 0) = \widehat{F}(\Omega_1, \mathbf{X}_1) \overline{\widehat{F}(\Omega_2, \mathbf{X}_2)}. \quad (4.36)$$

Here we used the notation $k_j = k(\Omega_j)$, for $j = 1, 2$.

The next proposition, proved in Appendix C, gives the approximation of \mathcal{C} in the strongly fluctuation regime (4.17). Since we have already described the spatial decorrelation of the wave field in the previous section, we give the approximation at the axis of the beam.

PROPOSITION 4.5. *In the regime (4.17), the decoherence frequency*

$$\Omega_\psi(z; \Omega) = \frac{2\Omega}{Q(z)R(z)} \quad (4.37)$$

is the scale of variation of the covariance of ψ with respect to the frequency offset $\Omega_1 - \Omega_2$ around the frequency Ω . More exactly, the covariance evaluated at $\mathbf{X}_1 = \mathbf{X}_2 = \mathbf{0}$ and at two positive frequencies Ω_1, Ω_2 such that $|\Omega_1 - \Omega_2| \lesssim \Omega_\psi(z; \Omega)$ with $\Omega = (\Omega_1 + \Omega_2)/2$ is of the form

$$\mathcal{C}(\Omega_1, \Omega_2, \mathbf{0}, \mathbf{0}, z) \simeq \frac{\widehat{\mathcal{F}}(\Omega_1, \Omega_2)}{R^2(z)} \Xi_\alpha \left(\frac{\Omega_1 - \Omega_2}{\Omega_\psi(z; \Omega)} \right), \quad (4.38)$$

with

$$\widehat{\mathcal{F}}(\Omega_1, \Omega_2) = \int_{\mathbb{R}^2} d\mathbf{X} \widehat{F}(\Omega_1, \mathbf{X}) \overline{\widehat{F}(\Omega_2, \mathbf{X})}, \quad (4.39)$$

and Ξ_α is a function that depends only on α . It is defined in equation (4.41) below for dimensionless, $O(1)$ arguments.

The decoherence frequency $\Omega_\psi(z; \Omega)$ given by (4.37) is proportional to the central frequency Ω , but it is much smaller because $QR \gg 1$ by (4.17). To define Ξ_α , we introduce the dimensionless and $O(1)$ variables

$$\widetilde{\mathbf{X}} = \frac{\mathbf{X}}{R(z)}, \quad \widetilde{\boldsymbol{\kappa}} = \frac{\boldsymbol{\kappa}}{Q(z)}, \quad (4.40)$$

where we anticipate the range dependent radii of spatial and wave vector support of the covariance, using the results in subsection 4.2 and definitions (4.18-4.19). The range z is fixed here, and we introduce the dimensionless $\widetilde{z} \in [0, 1]$, so that $z\widetilde{z} \in [0, z]$. With this notation we have

$$\Xi_\alpha(\widetilde{k}) = \int_{\mathbb{R}^2} d\widetilde{\boldsymbol{\kappa}} \widetilde{\mathcal{W}}_\alpha(\widetilde{k}, \widetilde{\mathbf{X}} = \mathbf{0}, \widetilde{\boldsymbol{\kappa}}, \widetilde{z} = 1) \quad (4.41)$$

for dimensionless and $O(1)$ variable \widetilde{k} , where $\widetilde{\mathcal{W}}_\alpha$ satisfies

$$\begin{aligned} [\partial_{\widetilde{z}} + (1 + \alpha)^{1/\alpha} \widetilde{\boldsymbol{\kappa}} \cdot \nabla_{\widetilde{\mathbf{X}}}] \widetilde{\mathcal{W}}_\alpha(\widetilde{k}, \widetilde{\mathbf{X}}, \widetilde{\boldsymbol{\kappa}}, \widetilde{z}) &= \frac{2^\alpha \alpha \Gamma(1 + \alpha/2)}{8\pi \Gamma(1 - \alpha/2)} \int_{\mathbb{R}^2} d\widetilde{\mathbf{q}} |\widetilde{\mathbf{q}}|^{-\alpha-2} \\ &\times [\widetilde{\mathcal{W}}_\alpha(\widetilde{k}, \widetilde{\mathbf{X}}, \widetilde{\boldsymbol{\kappa}} - \widetilde{\mathbf{q}}, \widetilde{z}) e^{-i\widetilde{k}\widetilde{\mathbf{q}} \cdot \widetilde{\mathbf{X}}} - \widetilde{\mathcal{W}}_\alpha(\widetilde{k}, \widetilde{\mathbf{X}}, \widetilde{\boldsymbol{\kappa}}, \widetilde{z})], \end{aligned} \quad (4.42)$$

at $\widetilde{z} > 0$, with initial condition

$$\widetilde{\mathcal{W}}_\alpha(\widetilde{k}, \widetilde{\mathbf{X}}, \widetilde{\boldsymbol{\kappa}}, \widetilde{z} = 0) = \delta(\widetilde{\mathbf{X}}) \delta(\widetilde{\boldsymbol{\kappa}}). \quad (4.43)$$

By scaling out the range z , the beam radius R and the wave vector radius Q , we made $\widetilde{\mathcal{W}}_\alpha$ and thus Ξ_α depend only on α . Note that when $\tilde{k} = 0$, which corresponds to taking $\Omega_1 = \Omega_2 = \Omega$ in (4.38), we recover the result in Proposition 4.4. Indeed, (4.39) becomes $\widehat{\mathcal{W}}_{\Omega,0}(\mathbf{0}, \mathbf{0})$, per definition (4.15), and solving explicitly (4.42) with a calculation similar to that in Appendix A, we get

$$\widetilde{\mathcal{W}}_\alpha(\tilde{k} = 0, \widetilde{\mathbf{X}}, \tilde{\boldsymbol{\kappa}}, \tilde{z} = 1) = \frac{1}{(2\pi)^2} \int_{\mathbb{R}^2} d\zeta \Phi_\alpha(\widetilde{\mathbf{X}}, \zeta) e^{-i\zeta \cdot \tilde{\boldsymbol{\kappa}}},$$

and

$$\Xi_\alpha(\tilde{k} = 0) = \int_{\mathbb{R}^2} d\tilde{\boldsymbol{\kappa}} \widetilde{\mathcal{W}}_\alpha(0, \mathbf{0}, \tilde{\boldsymbol{\kappa}}, 1) = \int_{\mathbb{R}^2} d\tilde{\boldsymbol{\kappa}} \frac{1}{(2\pi)^2} \int_{\mathbb{R}^2} d\zeta \Phi_\alpha(\mathbf{0}, \zeta) e^{-i\zeta \cdot \tilde{\boldsymbol{\kappa}}} = \Phi_\alpha(\mathbf{0}, \mathbf{0}).$$

4.4. Pulse deformation. The wave field evaluated at the center of the beam and observed around the central axis random travel time $z/c_o + \varepsilon^4 \mathcal{Z}^\varepsilon(z)/c_o$ is

$$\begin{aligned} U^\varepsilon(T, z) &= u^\varepsilon\left(t = \frac{z}{c_o} + \varepsilon^4 \frac{\mathcal{Z}^\varepsilon(z)}{c_o} + \varepsilon^4 T, \mathbf{x} = \mathbf{0}, z\right) \\ &= \frac{c_o}{4\pi} \int_{\mathbb{R}} d\Omega \psi^\varepsilon(\Omega, \mathbf{0}, z) e^{-i\Omega T}. \end{aligned} \quad (4.44)$$

In the limit $\varepsilon \rightarrow 0$ it converges in distribution to

$$U(T, z) = \frac{c_o}{4\pi} \int_{\mathbb{R}} d\Omega \psi(\Omega, \mathbf{0}, z) e^{-i\Omega T}, \quad (4.45)$$

where ψ is the solution of the Itô-Schrödinger equation (3.14) with the initial condition (3.15).

If the source has the Gaussian spectrum

$$\widehat{F}(\Omega, \mathbf{X}) = \frac{1}{B} \left[\exp\left(-\frac{(\Omega - \omega_o)^2}{2B^2}\right) + \exp\left(-\frac{(\Omega + \omega_o)^2}{2B^2}\right) \right] S\left(\frac{\mathbf{X}}{r_s}\right),$$

then the time-dependent wave field has the form

$$U(T, z) = e^{-i\omega_o T} \widetilde{U}(T, z) + c.c. \quad (4.46)$$

Here “c.c.” is short notation for the complex conjugate of the first term,

$$\widetilde{U}(T, z) = \frac{c_o}{4\pi} \int_{\mathbb{R}} e^{-i(\Omega - \omega_o)T} \widetilde{\psi}(\Omega, \mathbf{0}, z) d\Omega, \quad (4.47)$$

and the field $\widetilde{\psi}$ solves the same equation (3.14) as ψ , but has the initial condition

$$\widetilde{\psi}(\Omega, \mathbf{X}, z = 0) = \frac{1}{B} \exp\left(-\frac{(\Omega - \omega_o)^2}{2B^2}\right) S\left(\frac{\mathbf{X}}{r_s}\right).$$

To characterize the pulse profile, let us introduce the mean time-dependent intensity envelope

$$\begin{aligned} I(T, z) &= \mathbb{E}[|\widetilde{U}(T, z)|^2] \\ &= \frac{c_o^2}{(4\pi)^2} \int_{\mathbb{R}} d\Omega_1 \int_{\mathbb{R}} d\Omega_2 e^{-i(\Omega_1 - \Omega_2)T} \mathbb{E}[\widetilde{\psi}(\Omega_1, \mathbf{0}, z) \overline{\widetilde{\psi}(\Omega_2, \mathbf{0}, z)}]. \end{aligned}$$

In view of Proposition 4.5, if the condition (4.17) holds and the bandwidth satisfies $B \lesssim \Omega_\psi(z; \omega_o)$, then we get

$$I(T, z) = \frac{c_o^2}{16\pi^{3/2}} \frac{\int_{\mathbb{R}^2} d\mathbf{X} |S(\mathbf{X}/r_s)|^2}{BR^2(z)} \int_{\mathbb{R}} d\Omega e^{-\frac{\Omega^2}{4B^2} - iT\Omega} \Xi_\alpha\left(\frac{\Omega}{\Omega_\psi(z; \omega_o)}\right). \quad (4.48)$$

This result shows that the pulse profile is affected by the random medium via the function Ξ_α . For a narrowband pulse, with $B \ll \Omega_\psi(z, \omega_o)$, the profile is preserved and we have

$$I(T, z) = \frac{c_o^2}{2\pi} \frac{\int_{\mathbb{R}^2} d\mathbf{X} |S(\mathbf{X}/r_s)|^2}{R^2(z)} \Phi_\alpha(\mathbf{0}, \mathbf{0}) \exp(-B^2 T^2).$$

It is only when B is of the same order as $\Omega_\psi(z, \omega_o)$ that the random medium induces pulse deformation.

5. Comparison with the results in optics. In this section we compare the expression of the mean intensity and spectrum of the wave emerging from the asymptotic paraxial theory in random media and compare it with the results used in the optics literature [1]. Because this literature considers time-harmonic waves, we limit the comparison to a fixed frequency Ω .

We analyzed the spatial covariance \mathcal{C}_Ω in subsection 4.2 for $\alpha \in (0, 1)$ and $L_o \rightarrow \infty$, where the process μ has long-range correlations. We showed there that the central phase $k(\Omega)\mathcal{Z}^\varepsilon$, which is influenced by such correlations, plays no role i.e., \mathcal{C}_Ω is the covariance of ψ , the $\varepsilon \rightarrow 0$ limit (in distribution) of the wave field ψ^ε observed in the random travel time frame. Since ψ^ε experiences the random medium via the mixing process (3.10), the results in subsection 4.2 extend verbatim to the case $\alpha \in (0, 1) \cup (1, 2)$ and a finite L_o (recall subsection 2.2). In particular, the results (4.20), (4.25) and (4.26) remain valid as long as

$$R(z) < L_o, \quad Q(z) < l_o^{-1}. \quad (5.1)$$

The formulas in [1] are for the Kolmogorov spectrum of turbulence, corresponding to $\alpha = 5/3$. The radius R of the beam and the spectral radius Q for this α are, from definitions (4.18-4.19),

$$R(z) = \left(\frac{3}{8}d_{5/3}\right)^{3/5} z^{8/5} k^{1/5}(\Omega), \quad Q(z) = (d_{5/3})^{3/5} z^{3/5} k^{6/5}(\Omega), \quad (5.2)$$

and $d_{5/3}$ can be written in terms of the normalization constant $\chi_{5/3}$ of the random process μ using equation (4.8)

$$d_{5/3} = \frac{3\Gamma(1/6)}{5\pi 2^{8/3}\Gamma(11/6)} \chi_{5/3} \approx 0.178\chi_{5/3}. \quad (5.3)$$

To compare with the formulas in [1], we note that in [1, Section 3.3.1] the power spectrum of the fluctuations $\tilde{\mu}$ of the index of refraction is[†]

$$\mathbb{S}^{\text{A-P}}(\boldsymbol{\kappa}) = 0.033C_n^2 |\boldsymbol{\kappa}|^{-11/3} \mathbf{1}_{(L_o^{-1}, l_o^{-1})}(|\boldsymbol{\kappa}|). \quad (5.4)$$

[†]The power spectrum is called Φ_n in [1], but to avoid confusion with the function (4.27) we rename it $\mathbb{S}^{\text{A-P}}$.

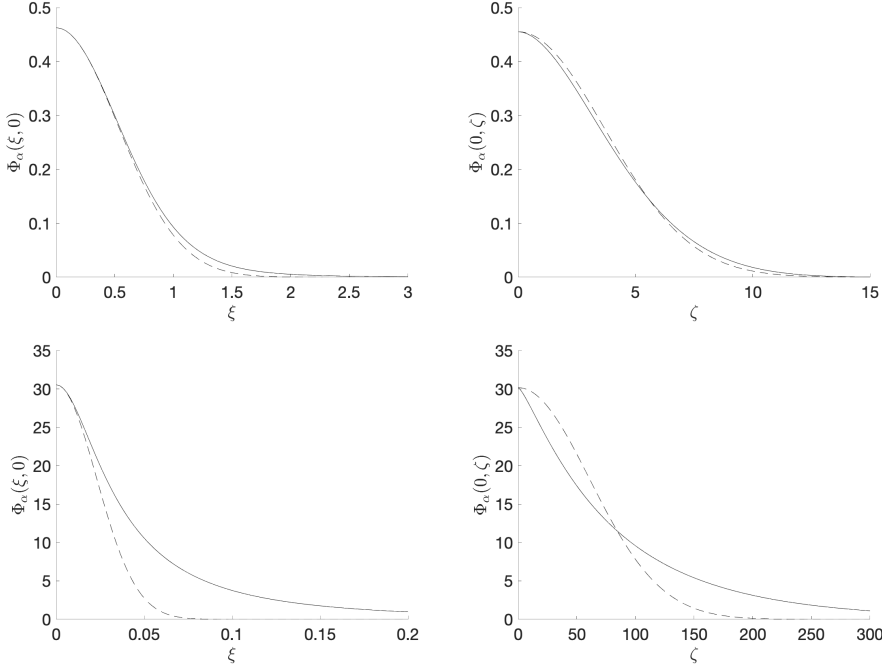


FIG. 5.1. *Left: Function $\xi \mapsto \Phi_\alpha(\xi, \mathbf{0})$ (solid line) and the Gaussian fit $\xi \mapsto \Phi_\alpha(\mathbf{0}, \mathbf{0}) \exp(-q_\alpha |\xi|^2)$ (dashed line; remember by (4.23) that $\Phi_\alpha(\xi, \mathbf{0}) = \Phi_\alpha(\mathbf{0}, \mathbf{0}) [1 - q_\alpha |\xi|^2 + o(|\xi|^2)]$). Right: Function $\zeta \mapsto \Phi_\alpha(\mathbf{0}, \zeta)$ (solid line) with the Gaussian fit $\zeta \mapsto \Phi_\alpha(\mathbf{0}, \mathbf{0}) \exp(-|\zeta|^2/\zeta_\alpha^2)$ (dashed line, with $\zeta_{2/3} = 86$ and $\zeta_{5/3} = 5.2$ determined by least-square fit). Top plots: $\alpha = 5/3$. Here the Gaussian fits are close to the true profiles. Bottom plots: $\alpha = 2/3$. Here the Gaussian fits are far from the true profiles, which have heavy tails.*

Since our process μ models the fluctuations of the squared index of refraction, we have $\mu \approx 2\tilde{\mu}$. We also have a different convention of the Fourier transform, which can be reconciled by dividing the formulas in [1] by $(2\pi)^3$. Then, we obtain from definition (1.2) that our power spectrum \mathbb{S} corresponds to (5.4) at $\alpha = 5/3$, for the normalization constant $\chi_{5/3} = 4(2\pi)^3 0.033C_n^2$, which gives, from (5.3),

$$d_{5/3} \approx 5.828C_n^2. \quad (5.5)$$

We begin the comparison with the mean intensity, which is proportional to $\Psi_\alpha(\mathbf{X}/R) = \Phi_\alpha(\mathbf{X}/R, \mathbf{0})$ per equations (4.20) and (4.26). This is approximated in [1, Section 7.3.3] by a Gaussian function, which is close to the true profile for $\alpha = 5/3$, as illustrated in the top left plot of Fig. 5.1. In this figure, the standard deviation of the Gaussian is $(2q_{5/3})^{-1/2}$ and $q_{5/3}$ can be determined from the expansion (4.23) of $\Psi_{5/3}$ about the origin: $q_{5/3} = \frac{2^{2/5}\Gamma(12/5)}{\Gamma(6/5)} \approx 1.785$. The radius of the support of the mean intensity defined in [1, Section 7.3.3], aka the “effective spotsize”, corresponds to

$$\frac{R(z)}{\sqrt{q_{5/3}}} \approx \frac{\left(\frac{3}{8} 5.828C_n^2\right)^{3/5}}{\sqrt{1.785}} z^{8/5} k^{1/5}(\Omega) \approx 1.2C_n^{6/5} z^{8/5} k^{1/5}(\Omega), \quad (5.6)$$

where we used equations (5.2-5.3). The effective spotsize is called W_{LT} in [1] and its estimate follows from equations (35) and (45) in Section 7.3.3 and the “Rytov

variance” given in Section 7.1. It is given by $1.45C_n^{6/5}z^{8/5}k^{1/5}$, which looks like the theoretically derived formula (5.6), except for the multiplicative constant. Thus, the effective spotsize seems to be slightly over-estimated in [1].

Similarly, we can quantify the “correlation radius”, which is defined in [1] as the radius of support of the mean spectrum, which is according to equations (4.25-4.26) proportional to $\Psi_{5/3}(\boldsymbol{\kappa}/Q) = \Phi_{5/3}(\mathbf{0}, \boldsymbol{\kappa}/Q)$. This is also modeled as Gaussian in [1], which is close to the true profile for the standard deviation $\zeta_{5/3}/\sqrt{2}$, $\zeta_{5/3} \approx 5.2$ (determined by least-square fit), as illustrated in the top right plot of Fig. 5.1. The correlation radius is

$$\frac{\zeta_{5/3}}{Q(z)} \approx \frac{\zeta_{5/3}}{(5.828C_n^2)^{3/5}} z^{-3/5} k^{-6/5}(\Omega) \approx 1.81C_n^{-6/5} z^{-3/5} k^{-6/5}(\Omega), \quad (5.7)$$

where we used equations (5.2-5.3). This is called ρ_{pl} in [1, Section 7.3.4] and it is estimated by $1.6C_n^{-6/5} z^{-3/5} k^{-6/5}(\Omega)$. Again, we see the similarity with the theoretically derived formula (5.7), except for the multiplicative constant that is slightly under-estimated.

Finally, we note that the Gaussian approximations of the mean intensity and spectrum are inadequate for the case $\alpha < 1$, as illustrated in the bottom plots of Fig. 5.1. The theoretically derived formulas (4.20) and (4.25) display heavier tails than the best fit Gaussian profiles.

6. Summary. Kolmogorov’s theory for optical turbulence predicts a power law form for the spectrum of the fluctuations of the index of refraction. In recent years, there has been a shift of focus on non-Kolmogorov turbulence. This is motivated in part by the analysis of atmospheric temperature recordings which show deviations from the Kolmogorov power spectrum. However, these studies deal mostly with the case of light tails of the two-point statistics for the medium fluctuations, which correspond to an integrable covariance function. Here we consider beam wave propagation in random media with long-range correlations, where the tails of the covariance function decay at a slower rate and the medium contains more features of low spatial frequency. We explicitly discuss the roles of the inner and outer scales delineating the power law, and contrast the results with those for the Kolmogorov turbulence.

A main result in the long-range case is that the randomization of the wave field is multiscale: First, we show that as the beam wave propagates through the medium, a strong random travel time perturbation builds up. We present a precise characterization of the travel time perturbation, which corresponds to a fractional Brownian motion, with Hurst index and amplitude determined by the statistics of the medium. Second, we show that if we observe the beam wave at large propagation distances where the travel time correction is large relative to the pulse width, then the beam wave pulse shape itself is deformed and becomes random due to scattering.

Another important result is a detailed characterization of the decorrelation of the random beam wave both in space and frequency. This is carried out in the random travel time centered frame because otherwise, the frequency decorrelation would be masked by the very large random phase associated with the travel time fluctuations. The analysis reveals a cusp like behavior for the spatial correlations of the wave field in the transverse coordinates, with the cusp shape depending on the rate of decay of the covariance of the medium fluctuations. The scale of frequency decorrelation is also quantified and it is used to analyze the deformation of the probing pulse induced by scattering.

The results of our analysis are important for applications like imaging and communication through the atmosphere, and also for propagation through the earth's crust or through the ocean. In the case of communication applications a characterization of the statistics of fading or strong pulse deformation is important in order to evaluate the efficiency of various communication protocols. In imaging through complex media, one needs to take into account the geometric wavefront distortion that is caused by the random travel time as well as the deformation or blurring of the beam pulse shape. Quantitative insights about these effects are useful when designing schemes for clutter and turbulence compensation.

Acknowledgements. This material is based upon work supported by the Air Force Office of Scientific Research under award numbers FA9550-22-1-0077 and FA9550-22-1-0176, by the U.S. Office of Naval Research under award number N00014-21-1-2370 and by the National Science Foundation under grant DMS-2010046.

Appendix A. Proof of Proposition 4.1. Equation (4.10) written in the coordinates (4.12) is

$$\partial_z \mathcal{C}_\Omega \left(\mathbf{X} + \frac{\mathbf{Y}}{2}, \mathbf{X} - \frac{\mathbf{Y}}{2}, z \right) = \left[\frac{i}{k(\Omega)} \nabla_{\mathbf{X}} \cdot \nabla_{\mathbf{Y}} - \frac{k^2(\Omega)}{4} \Theta(\mathbf{Y}) \right] \mathcal{C}_\Omega \left(\mathbf{X} + \frac{\mathbf{Y}}{2}, \mathbf{X} - \frac{\mathbf{Y}}{2}, z \right), \quad (\text{A.1})$$

and using the Fourier transform

$$\widehat{\mathcal{W}}_\Omega(\mathbf{q}, \mathbf{Y}, z) = \int_{\mathbb{R}^2} d\mathbf{X} \mathcal{C}_\Omega \left(\mathbf{X} + \frac{\mathbf{Y}}{2}, \mathbf{X} - \frac{\mathbf{Y}}{2}, z \right) e^{-i\mathbf{q} \cdot \mathbf{X}}, \quad (\text{A.2})$$

we get

$$\left(\partial_z + \frac{\mathbf{q}}{k(\Omega)} \cdot \nabla_{\mathbf{Y}} \right) \widehat{\mathcal{W}}_\Omega(\mathbf{q}, \mathbf{Y}, z) = -\frac{k^2(\Omega)}{4} \Theta(\mathbf{Y}) \widehat{\mathcal{W}}_\Omega(\mathbf{q}, \mathbf{Y}, z), \quad (\text{A.3})$$

for $z > 0$, with initial condition $\widehat{\mathcal{W}}_\Omega(\mathbf{q}, \mathbf{Y}, 0) = \widehat{\mathcal{W}}_{\Omega,0}(\mathbf{q}, \mathbf{Y})$, defined in (4.15).

We can solve (A.3) by integration along the characteristic $\mathbf{Y} = \mathbf{Y}_0 + \mathbf{q}z/k(\Omega)$, starting from \mathbf{Y}_0 , using that

$$\begin{aligned} \partial_z \widehat{\mathcal{W}}_\Omega \left(\mathbf{q}, \mathbf{Y}_0 + \frac{\mathbf{q}}{k(\Omega)} z, z \right) &= \left(\partial_z + \frac{\mathbf{q}}{k(\Omega)} \cdot \nabla_{\mathbf{Y}} \right) \mathcal{W}_\Omega \left(\mathbf{q}, \mathbf{Y}_0 + \frac{\mathbf{q}}{k(\Omega)} z, z \right) \\ &= -\frac{k^2(\Omega)}{4} \Theta(\mathbf{Y}) \mathcal{W}_\Omega \left(\mathbf{q}, \mathbf{Y}_0 + \frac{\mathbf{q}}{k(\Omega)} z, z \right), \quad z > 0. \end{aligned}$$

The result is

$$\widehat{\mathcal{W}}_\Omega \left(\mathbf{q}, \mathbf{Y}_0 + \frac{\mathbf{q}}{k(\Omega)} z, z \right) = \widehat{\mathcal{W}}_{\Omega,0}(\mathbf{q}, \mathbf{Y}_0) \exp \left[-\frac{k^2(\Omega)}{4} \int_0^z dz' \Theta \left(\mathbf{Y}_0 + \frac{\mathbf{q}}{k(\Omega)} z' \right) \right],$$

or, equivalently, in terms of \mathbf{Y} ,

$$\widehat{\mathcal{W}}_\Omega(\mathbf{q}, \mathbf{Y}, z) = \widehat{\mathcal{W}}_{\Omega,0} \left(\mathbf{q}, \mathbf{Y} - \frac{\mathbf{q}}{k(\Omega)} z \right) \exp \left[-\frac{k^2(\Omega)}{4} \int_0^z dz' \Theta \left(\mathbf{Y} - \frac{\mathbf{q}}{k(\Omega)} (z - z') \right) \right].$$

The result stated in Proposition 4.1 follows from this expression and the definition

(4.13) of the Wigner transform,

$$\begin{aligned}
\mathcal{W}_\Omega(\mathbf{X}, \boldsymbol{\kappa}, z) &= \int_{\mathbb{R}^2} d\mathbf{Y} \mathcal{C}_\Omega\left(\mathbf{X} + \frac{\mathbf{Y}}{2}, \mathbf{X} - \frac{\mathbf{Y}}{2}, z\right) \exp(-i\boldsymbol{\kappa} \cdot \mathbf{Y}) \\
&= \int_{\mathbb{R}^2} d\mathbf{Y} \int_{\mathbb{R}^2} \frac{d\mathbf{q}}{(2\pi)^2} \widehat{\mathcal{W}}_\Omega(\mathbf{q}, \mathbf{Y}, z) \exp(i\mathbf{q} \cdot \mathbf{X} - i\boldsymbol{\kappa} \cdot \mathbf{Y}) \\
&= \frac{1}{(2\pi)^2} \int_{\mathbb{R}^2} d\mathbf{q} \int_{\mathbb{R}^2} d\mathbf{Y} \widehat{\mathcal{W}}_{\Omega,0}\left(\mathbf{q}, \mathbf{Y} - \frac{\mathbf{q}}{k(\Omega)}z\right) \exp(i\mathbf{q} \cdot \mathbf{X} - i\boldsymbol{\kappa} \cdot \mathbf{Y}) \\
&\quad \times \exp\left[-\frac{k^2(\Omega)}{4} \int_0^z dz' \Theta\left(\mathbf{Y} - \frac{\mathbf{q}}{k(\Omega)}(z - z')\right)\right].
\end{aligned}$$

In (4.14) we used the change of variable $\mathbf{Y}' = \mathbf{Y} - \frac{\mathbf{q}}{k(\Omega)}z$. \square

Appendix B. Proof of the expansion (4.29). We first remark that

$$|\mathbf{y}|^\alpha - |\mathbf{x}|^\alpha = \mathfrak{C}_\alpha \int_{\mathbb{R}^2} d\mathbf{q} |\mathbf{q}|^{-\alpha-2} (e^{i\mathbf{q} \cdot \mathbf{x}} - e^{i\mathbf{q} \cdot \mathbf{y}}),$$

with constant \mathfrak{C}_α defined by

$$\mathfrak{C}_\alpha^{-1} = 2\pi \int_0^\infty (1 - J_0(s)) s^{-1-\alpha} ds.$$

Next, we compute from (4.27):

$$\Phi_\alpha(\mathbf{0}, \boldsymbol{\zeta}) - \Phi_\alpha(\mathbf{0}, \mathbf{0}) = -\Phi_{\alpha,1}(\boldsymbol{\zeta})(1 + o(1)), \quad (\text{B.1})$$

with

$$\begin{aligned}
\Phi_{\alpha,1}(\boldsymbol{\zeta}) &= \frac{1}{4(2\pi)^2} \int_{\mathbb{R}^2} d\boldsymbol{\eta} e^{-\frac{1}{4}|\boldsymbol{\eta}|^\alpha} \int_0^1 ds (|\boldsymbol{\zeta} - (1+\alpha)^{1/\alpha} \boldsymbol{\eta} s|^\alpha - |(1+\alpha)^{1/\alpha} \boldsymbol{\eta} s|^\alpha) \\
&= \frac{\mathfrak{C}_\alpha}{4(2\pi)^2} \int_{\mathbb{R}^2} d\boldsymbol{\eta} e^{-\frac{1}{4}|\boldsymbol{\eta}|^\alpha} \int_0^1 ds \int_{\mathbb{R}^2} d\mathbf{q} |\mathbf{q}|^{-\alpha-2} e^{i(1+\alpha)^{1/\alpha} \boldsymbol{\eta} \cdot \mathbf{q} s} (1 - e^{-i\boldsymbol{\zeta} \cdot \mathbf{q}}) \\
&= \frac{\mathfrak{C}_\alpha}{4} \int_0^\infty d\boldsymbol{\eta} \boldsymbol{\eta} e^{-\frac{1}{4}|\boldsymbol{\eta}|^\alpha} \int_0^1 ds \int_0^\infty dq q^{-\alpha-1} J_0((1+\alpha)^{1/\alpha} \boldsymbol{\eta} q s) (1 - J_0(|\boldsymbol{\zeta}|q)) \\
&= \frac{\mathfrak{C}_\alpha}{4(1+\alpha)^{1/\alpha}} \int_0^\infty d\boldsymbol{\eta} \boldsymbol{\eta} e^{-\frac{1}{4}|\boldsymbol{\eta}|^\alpha} \int_0^\infty dq q^{-\alpha-2} \mathcal{J}_0((1+\alpha)^{1/\alpha} \boldsymbol{\eta} q) (1 - J_0(|\boldsymbol{\zeta}|q)),
\end{aligned}$$

where $\mathcal{J}_o(s) = \int_0^s J_0(s') ds'$ is the antiderivative of the Bessel function J_0 . It is a bounded function that converges to one as $s \rightarrow +\infty$. By the change of variable $s = |\boldsymbol{\zeta}|q$, we get

$$\Phi_{\alpha,1}(\boldsymbol{\zeta}) = \frac{C_\alpha |\boldsymbol{\zeta}|^{\alpha+1}}{4(1+\alpha)^{1/\alpha}} \int_0^\infty d\boldsymbol{\eta} \boldsymbol{\eta} e^{-\frac{1}{4}|\boldsymbol{\eta}|^\alpha} \int_0^\infty ds s^{-\alpha-2} \mathcal{J}_0\left(\frac{(1+\alpha)^{1/\alpha} \boldsymbol{\eta} s}{|\boldsymbol{\zeta}|}\right) (1 - J_0(s)).$$

Using the dominated convergence theorem, we find

$$\frac{\Phi_{\alpha,1}(\boldsymbol{\zeta})}{|\boldsymbol{\zeta}|^{\alpha+1}} \xrightarrow{|\boldsymbol{\zeta}| \rightarrow 0} \frac{C_\alpha}{4(1+\alpha)^{1/\alpha}} \int_0^\infty d\boldsymbol{\eta} \boldsymbol{\eta} e^{-\frac{1}{4}|\boldsymbol{\eta}|^\alpha} \int_0^\infty ds s^{-\alpha-2} (1 - J_0(s)).$$

Therefore, equation (B.1) gives the expansion

$$\Phi_\alpha(\mathbf{0}, \boldsymbol{\zeta}) = \Phi_\alpha(\mathbf{0}, \mathbf{0}) (1 - r_\alpha |\boldsymbol{\zeta}|^{\alpha+1} + o(|\boldsymbol{\zeta}|^{\alpha+1})),$$

with

$$r_\alpha = \frac{\int_0^\infty d\eta e^{-\frac{1}{4}\eta^\alpha} \int_0^\infty ds s^{-\alpha-2} (1 - J_0(s)) ds}{8\pi(1 + \alpha)^{1/\alpha} \Phi_\alpha(\mathbf{0}, \mathbf{0}) \int_0^\infty s^{-\alpha-1} (1 - J_0(s))}.$$

The desired result follows once we use

$$\Phi_\alpha(\mathbf{0}, \mathbf{0}) = \frac{1}{2\pi} \int_0^\infty d\eta \eta e^{-\frac{1}{4}\eta^\alpha},$$

and the identities

$$\begin{aligned} \int_0^\infty ds s^{-\alpha-1} (1 - J_0(s)) &= \frac{2^{-\alpha} \Gamma(1 - \alpha/2)}{\alpha \Gamma(1 + \alpha/2)}, \\ \int_0^\infty ds s^{-\alpha-2} (1 - J_0(s)) &= \frac{2^{-\alpha-1} \Gamma(1/2 - \alpha/2)}{\alpha + 1 \Gamma(3/2 + \alpha/2)}, \\ \int_0^\infty d\eta \eta e^{-\frac{1}{4}\eta^\alpha} &= \frac{2^{4/\alpha}}{\alpha} \Gamma\left(\frac{2}{\alpha}\right), \\ \int_0^\infty d\eta e^{-\frac{1}{4}\eta^\alpha} &= \frac{2^{2/\alpha}}{\alpha} \Gamma\left(\frac{1}{\alpha}\right). \end{aligned}$$

Appendix C. Proof of Proposition 4.5. Let us introduce the reference wavenumber k and use it to change coordinates in the cross-range plane, as follows

$$\mathbf{X}_1 = \sqrt{\frac{k}{k_1}} \left(\mathbf{X} + \frac{\mathbf{Y}}{2} \right), \quad \mathbf{X}_2 = \sqrt{\frac{k}{k_2}} \left(\mathbf{X} - \frac{\mathbf{Y}}{2} \right). \quad (\text{C.1})$$

Writing the evolution equation (4.35) in these coordinates and then taking the Fourier transform in \mathbf{Y} , which defines the Wigner transform

$$\mathcal{W}(\Omega_1, \Omega_2, \mathbf{X}, \boldsymbol{\kappa}, z) = \int_{\mathbb{R}^2} d\mathbf{Y} \mathcal{C}(\Omega_1, \Omega_2, \sqrt{\frac{k}{k_1}} \left(\mathbf{X} + \frac{\mathbf{Y}}{2} \right), \sqrt{\frac{k}{k_2}} \left(\mathbf{X} - \frac{\mathbf{Y}}{2} \right), z) e^{-i\boldsymbol{\kappa} \cdot \mathbf{Y}},$$

we obtain the following equation

$$\begin{aligned} \left(\partial_z + \frac{1}{k} \boldsymbol{\kappa} \cdot \nabla_{\mathbf{X}} \right) \mathcal{W}(\Omega_1, \Omega_2, \mathbf{X}, \boldsymbol{\kappa}, z) &= -\frac{1}{4(2\pi)^2} \int_{\mathbb{R}^2} d\mathbf{q} \hat{\Theta}(\mathbf{q}) \\ &\times \left\{ k_1 k_2 \mathcal{W} \left(\Omega_1, \Omega_2, \mathbf{X}, \boldsymbol{\kappa} - \frac{\mathbf{q}}{2} \left(\sqrt{\frac{k}{k_1}} + \sqrt{\frac{k}{k_2}} \right), z \right) e^{i\mathbf{X} \cdot \mathbf{q} \left(\sqrt{\frac{k}{k_1}} - \sqrt{\frac{k}{k_2}} \right)} \right. \\ &+ k_1 (k_1 - k_2) \mathcal{W} \left(\Omega_1, \Omega_2, \mathbf{X}, \boldsymbol{\kappa} - \frac{\mathbf{q}}{2} \sqrt{\frac{k}{k_1}}, z \right) e^{i\mathbf{X} \cdot \mathbf{q} \sqrt{\frac{k}{k_1}}} \\ &\left. - k_2 (k_1 - k_2) \mathcal{W} \left(\Omega_1, \Omega_2, \mathbf{X}, \boldsymbol{\kappa} + \frac{\mathbf{q}}{2} \sqrt{\frac{k}{k_2}}, z \right) e^{i\mathbf{X} \cdot \mathbf{q} \sqrt{\frac{k}{k_2}}} \right\}, \quad (\text{C.2}) \end{aligned}$$

for $z > 0$, where the net effect of the random medium is in the Fourier transform $\hat{\Theta}$ of the function Θ defined in (4.7).

Although we are interested in an infinite outer scale, let us consider a modification of (4.7), corresponding to a finite L_o ,

$$\Theta_{L_o}(\mathbf{X}) = \frac{\chi_\alpha}{2\pi} \int_{L_o^{-1}}^{L_o^{-1}} d\kappa [1 - J_0(\kappa|\mathbf{X}|)] \kappa^{-1-\alpha} = \Theta(\mathbf{X}) + O\left(\frac{\chi_\alpha |\mathbf{X}|^2}{L_o^{2-\alpha}}\right) \xrightarrow{L_o \rightarrow \infty} \Theta(\mathbf{X}).$$

The Fourier transform of this function is

$$\widehat{\Theta}_{L_o}(\mathbf{q}) = \int_{\mathbb{R}^2} d\mathbf{X} \Theta_{L_o}(\mathbf{X}) e^{-i\mathbf{q}\cdot\mathbf{X}} = 2\pi\chi_\alpha \frac{(L_o^\alpha - l_o^\alpha)}{\alpha} \delta(\mathbf{q}) - \chi_\alpha |\mathbf{q}|^{-2-\alpha} \mathbf{1}_{(L_o^{-1}, l_o^{-1})}(|\mathbf{q}|)$$

and we explain next that equation (C.2) makes sense for $L_o \rightarrow \infty$. Using the observation

$$\int_{\mathbb{R}^2} d\mathbf{q} \mathbf{1}_{(L_o^{-1}, l_o^{-1})}(|\mathbf{q}|) |\mathbf{q}|^{-2-\alpha} = 2\pi \int_0^\infty dq \mathbf{1}_{(L_o^{-1}, l_o^{-1})}(q) q^{-1-\alpha} = \frac{2\pi(L_o^\alpha - l_o^\alpha)}{\alpha},$$

we can rewrite (C.2), with $\widehat{\Theta}$ replaced by $\widehat{\Theta}_{L_o}$ and therefore \mathcal{W} replaced by \mathcal{W}_{L_o} as follows

$$\begin{aligned} \left(\partial_z + \frac{1}{k} \boldsymbol{\kappa} \cdot \nabla_{\mathbf{X}} \right) \mathcal{W}_{L_o}(\Omega_1, \Omega_2, \mathbf{X}, \boldsymbol{\kappa}, z) &= \frac{\chi_\alpha}{4(2\pi)^2} \int_{\mathbb{R}^2} d\mathbf{q} \mathbf{1}_{(L_o^{-1}, l_o^{-1})}(|\mathbf{q}|) |\mathbf{q}|^{-2-\alpha} \left\{ k_1 k_2 \right. \\ &\times \left[\mathcal{W}_{L_o} \left(\Omega_1, \Omega_2, \mathbf{X}, \boldsymbol{\kappa} - \frac{\mathbf{q}}{2} \left(\sqrt{\frac{k}{k_1}} + \sqrt{\frac{k}{k_2}} \right), z \right) e^{i\mathbf{X}\cdot\mathbf{q} \left(\sqrt{\frac{k}{k_1}} - \sqrt{\frac{k}{k_2}} \right)} - \mathcal{W}_{L_o}(\Omega_1, \Omega_2, \mathbf{X}, \boldsymbol{\kappa}, z) \right] \\ &+ k_1(k_1 - k_2) \left[\mathcal{W}_{L_o} \left(\Omega_1, \Omega_2, \mathbf{X}, \boldsymbol{\kappa} - \frac{\mathbf{q}}{2} \sqrt{\frac{k}{k_1}}, z \right) e^{i\mathbf{X}\cdot\mathbf{q} \sqrt{\frac{k}{k_1}}} - \mathcal{W}_{L_o}(\Omega_1, \Omega_2, \mathbf{X}, \boldsymbol{\kappa}, z) \right] \\ &\left. - k_2(k_1 - k_2) \left[\mathcal{W}_{L_o} \left(\Omega_1, \Omega_2, \mathbf{X}, \boldsymbol{\kappa} + \frac{\mathbf{q}}{2} \sqrt{\frac{k}{k_2}}, z \right) e^{i\mathbf{X}\cdot\mathbf{q} \sqrt{\frac{k}{k_2}}} - \mathcal{W}_{L_o}(\Omega_1, \Omega_2, \mathbf{X}, \boldsymbol{\kappa}, z) \right] \right\}. \end{aligned} \quad (\text{C.3})$$

At $|\mathbf{q}| \sim L_o^{-1} \rightarrow 0$ the square brackets in this expression are $O(|\mathbf{q}|)$, and after writing the \mathbf{q} integral in polar coordinates we conclude that the integrand is $O(|\mathbf{q}|^{-\alpha})$. Thus, after the integration in $|\mathbf{q}|$ the right-hand side depends on the outer scale as $L_o^{-(1-\alpha)}$. This vanishes as $L_o \rightarrow \infty$, so we can take the limit in (C.3) and replace \mathcal{W}_{L_o} by \mathcal{W} .

Since the integrand in (C.3) has a fast decay at $|\mathbf{q}| \rightarrow \infty$, like $|\mathbf{q}|^{-1-\alpha}$, and we are interested in a small inner scale (recall section 4.2), we can approximate \mathcal{W} by taking the limit $l_o \rightarrow 0$. We obtain the equation

$$\begin{aligned} \left(\partial_z + \frac{1}{k} \boldsymbol{\kappa} \cdot \nabla_{\mathbf{X}} \right) \mathcal{W}(\Omega_1, \Omega_2, \mathbf{X}, \boldsymbol{\kappa}, z) &= \frac{\chi_\alpha}{4(2\pi)^2} \int_{\mathbb{R}^2} d\mathbf{q} |\mathbf{q}|^{-2-\alpha} \left\{ k_1 k_2 \right. \\ &\times \left[\mathcal{W} \left(\Omega_1, \Omega_2, \mathbf{X}, \boldsymbol{\kappa} - \frac{\mathbf{q}}{2} \left(\sqrt{\frac{k}{k_1}} + \sqrt{\frac{k}{k_2}} \right), z \right) e^{i\mathbf{X}\cdot\mathbf{q} \left(\sqrt{\frac{k}{k_1}} - \sqrt{\frac{k}{k_2}} \right)} - \mathcal{W}(\Omega_1, \Omega_2, \mathbf{X}, \boldsymbol{\kappa}, z) \right] \\ &+ k_1(k_1 - k_2) \left[\mathcal{W} \left(\Omega_1, \Omega_2, \mathbf{X}, \boldsymbol{\kappa} - \frac{\mathbf{q}}{2} \sqrt{\frac{k}{k_1}}, z \right) e^{i\mathbf{X}\cdot\mathbf{q} \sqrt{\frac{k}{k_1}}} - \mathcal{W}(\Omega_1, \Omega_2, \mathbf{X}, \boldsymbol{\kappa}, z) \right] \\ &\left. - k_2(k_1 - k_2) \left[\mathcal{W} \left(\Omega_1, \Omega_2, \mathbf{X}, \boldsymbol{\kappa} + \frac{\mathbf{q}}{2} \sqrt{\frac{k}{k_2}}, z \right) e^{i\mathbf{X}\cdot\mathbf{q} \sqrt{\frac{k}{k_2}}} - \mathcal{W}(\Omega_1, \Omega_2, \mathbf{X}, \boldsymbol{\kappa}, z) \right] \right\}, \end{aligned} \quad (\text{C.4})$$

for $z > 0$, with the initial condition

$$\mathcal{W}(\Omega_1, \Omega_2, \mathbf{X}, \boldsymbol{\kappa}, 0) = \int_{\mathbb{R}^2} d\mathbf{Y} \widehat{F} \left(\Omega_1, \sqrt{\frac{k}{k_1}} \left(\mathbf{X} + \frac{\mathbf{Y}}{2} \right) \right) \overline{\widehat{F} \left(\Omega_2, \sqrt{\frac{k}{k_2}} \left(\mathbf{X} - \frac{\mathbf{Y}}{2} \right) \right)} e^{-i\boldsymbol{\kappa}\cdot\mathbf{Y}}. \quad (\text{C.5})$$

Let us consider a range Z in the strong fluctuation medium (4.17) so that we have $Q_Z R_Z \gg 1$ with

$$Q_Z = Q(Z) = (d_\alpha k^2 Z)^{1/\alpha}, \quad R_Z = R(Z) = \left(\frac{d_\alpha k^{2-\alpha} Z^{\alpha+1}}{\alpha + 1} \right)^{1/\alpha}. \quad (\text{C.6})$$

We now show that the decoherence frequency i.e., the scale of decay of \mathcal{W} with respect to $|\Omega_1 - \Omega_2|$ is $c_o K_Z$, where

$$K_Z = \frac{2k}{Q_Z R_Z} \ll k. \quad (\text{C.7})$$

Indeed, suppose that

$$k_j = k(\Omega_j) = k + K_Z \tilde{k}_j, \quad j = 1, 2, \quad (\text{C.8})$$

where \tilde{k}_j are dimensionless $O(1)$ scaled wavenumber offsets with respect to k . Then,

$$\frac{(k_1 + k_2)}{2} \simeq k \left[1 + O\left(\frac{1}{Q_Z R_Z}\right) \right],$$

and

$$k_1 - k_2 = K_Z(\tilde{k}_1 - \tilde{k}_2) = O(K_Z) \ll k.$$

Introduce also the dimensionless variables

$$\tilde{\mathbf{X}} = \frac{\mathbf{X}}{R_Z}, \quad \tilde{\mathbf{q}} = \frac{\mathbf{q}}{Q_Z}, \quad \tilde{\boldsymbol{\kappa}} = \frac{\boldsymbol{\kappa}}{Q_Z}, \quad \tilde{z} = \frac{z}{Z}. \quad (\text{C.9})$$

Then, the Wigner transform can be approximated by

$$\mathcal{W}(\Omega_1, \Omega_2, \mathbf{X}, \boldsymbol{\kappa}, z) \approx \frac{(2\pi)^2 \hat{\mathcal{F}}(\Omega_1, \Omega_2)}{(R_Z Q_Z)^2} \tilde{\mathcal{W}}(\tilde{k}_1 - \tilde{k}_2, \tilde{\mathbf{X}}, \tilde{\boldsymbol{\kappa}}, \tilde{z}), \quad (\text{C.10})$$

with $\hat{\mathcal{F}}$ defined in (4.39) and the function $\tilde{\mathcal{W}}$ of dimensionless $O(1)$ arguments satisfying equation (4.42), with initial condition (4.43).

To derive (4.42) we used definitions (C.6) and (4.8), which give

$$\partial_z + \frac{1}{k} \boldsymbol{\kappa} \cdot \nabla_{\mathbf{X}} = \frac{1}{Z} \left(\partial_{\tilde{z}} + \frac{Z Q_Z}{k R_Z} \tilde{\boldsymbol{\kappa}} \cdot \nabla_{\tilde{\mathbf{X}}} \right) = \frac{1}{Z} \left(\partial_{\tilde{z}} + (1 + \alpha)^{1/\alpha} \tilde{\boldsymbol{\kappa}} \cdot \nabla_{\tilde{\mathbf{X}}} \right), \quad (\text{C.11})$$

and

$$Z \chi_\alpha k^2 Q_Z^{-\alpha} = \frac{\chi_\alpha}{d_\alpha} = \frac{2^{\alpha+1} \pi \alpha \Gamma(1 + \alpha/2)}{\Gamma(1 - \alpha/2)}. \quad (\text{C.12})$$

We also used (C.7-C.8) and neglected the small, $O((\tilde{k}_1 - \tilde{k}_2) K_Z/k)$ residual.

To justify the initial condition (4.43) we note first that in the regime defined by (C.7-C.8) we have

$$\begin{aligned} \mathcal{W}(\Omega_1, \Omega_2, \mathbf{X}, \boldsymbol{\kappa}, 0) &\approx \frac{r_s^2}{B^2} \tilde{\mathcal{W}}_s \left(\frac{\tilde{\mathbf{X}}}{r_s/R_Z}, \frac{\tilde{\boldsymbol{\kappa}}}{1/(r_s Q_Z)} \right) \left[\hat{f} \left(\frac{\Omega_1 - \omega_o}{B} \right) + \hat{f} \left(\frac{\Omega_1 + \omega_o}{B} \right) \right] \\ &\times \left[\hat{f} \left(\frac{\Omega_2 - \omega_o}{B} \right) + \hat{f} \left(\frac{\Omega_2 + \omega_o}{B} \right) \right], \end{aligned} \quad (\text{C.13})$$

where

$$\tilde{\mathcal{W}}_s(\tilde{\mathbf{X}}, \tilde{\boldsymbol{\kappa}}) = \int_{\mathbb{R}^2} d\xi S(\tilde{\mathbf{X}} + \frac{\xi}{2}) \overline{S(\tilde{\mathbf{X}} - \frac{\xi}{2})} e^{-i\tilde{\boldsymbol{\kappa}} \cdot \xi} \quad (\text{C.14})$$

is the dimensionless Wigner transform of the source function S . Since $r_s/R_Z \ll 1$ and $1/(r_s Q_Z) \ll 1$ by (4.17) and (C.6), we conclude from (C.13-C.14) that the initial condition is supported at $\widetilde{\mathbf{X}} \approx \mathbf{0}$ and $\widetilde{\boldsymbol{\kappa}} \approx \mathbf{0}$. This is why we use the Dirac delta in (4.43). The normalization in (C.10) comes from the identity

$$\int_{\mathbb{R}^2} d\widetilde{\mathbf{X}} \int_{\mathbb{R}^2} d\widetilde{\boldsymbol{\kappa}} \mathcal{W}(\Omega_1, \Omega_2, R_Z \widetilde{\mathbf{X}}, Q_Z \widetilde{\boldsymbol{\kappa}}, 0) = \frac{(2\pi)^2}{(R_Z Q_Z)^2} \widehat{\mathcal{F}}(\Omega_1, \Omega_2), \quad (\text{C.15})$$

derived from (C.13-C.14), with $\widehat{\mathcal{F}}$ defined in (4.39).

REFERENCES

- [1] LC ANDREWS AND RL PHILLIPS, *Laser beam propagation through random media*, in SPIE-International Society for Optical Engineering, 2005. [1](#), [2](#), [17](#), [18](#), [19](#)
- [2] G BAL, T KOMOROWSKI, AND L RYZHIK, *Asymptotics of the solutions of the random schrödinger equation*, Archive for rational mechanics and analysis, 200 (2011), pp. 613–664. [2](#)
- [3] A BAMBERGER, B ENGQUIST, L HALPERN, AND P JOLY, *Parabolic wave equation approximations in heterogeneous media*, SIAM Journal on Applied Mathematics, 48 (1988), pp. 99–128. [1](#)
- [4] P BLOMGREN, G PAPANICOLAOU, AND H ZHAO, *Super-resolution in time-reversal acoustics*, The Journal of the Acoustical Society of America, 111 (2002), pp. 230–248. [2](#)
- [5] L BORCEA AND J GARNIER, *Imaging in random media by two-point coherent interferometry*, SIAM Journal on Imaging Sciences, 14 (2021), pp. 1635–1668. [2](#), [9](#)
- [6] L BORCEA, J GARNIER, G PAPANICOLAOU, AND C TSOGKA, *Enhanced statistical stability in coherent interferometric imaging*, Inverse problems, 27 (2011), p. 085004. [9](#), [10](#)
- [7] L BORCEA, J GARNIER, AND K SÖLNA, *Multimode communication through the turbulent atmosphere*, JOSA A, 37 (2020), pp. 720–730. [2](#)
- [8] L BORCEA, G PAPANICOLAOU, AND C TSOGKA, *Adaptive interferometric imaging in clutter and optimal illumination*, Inverse problems, 22 (2006), p. 1405. [9](#)
- [9] ———, *Asymptotics for the space-time Wigner transform with applications to imaging*, in Stochastic Differential Equations: Theory And Applications: A Volume in Honor of Professor Boris L Rozovskii, World Scientific, 2007, pp. 91–111. [2](#), [10](#)
- [10] RF CAHALAN AND JB SNIDER, *Marine stratocumulus structure*, Remote Sensing of Environment, 28 (1989), pp. 95–107. [2](#)
- [11] M CHARNOTSKII, *Intensity fluctuations of flat-topped beam in non-Kolmogorov weak turbulence: comment*, JOSA A, 29 (2012), pp. 1838–1840. [2](#)
- [12] JF CLAERBOUT, *Coarse grid calculations of waves in inhomogeneous media with application to delineation of complicated seismic structure*, Geophysics, 35 (1970), pp. 407–418. [1](#)
- [13] ———, *Fundamentals of geophysical data processing*, vol. 274, Citeseer, 1976. [1](#)
- [14] AC FANNJIANG AND K SÖLNA, *Scaling limits for beam wave propagation in atmospheric turbulence*, Stochastics and Dynamics, 4 (2004), pp. 135–151. [2](#), [4](#), [8](#)
- [15] ———, *Propagation and time-reversal of wave beams in atmospheric turbulence*, SIAM Journal on Multiscale Modeling and Simulation, 3 (2005), pp. 522–558. [2](#)
- [16] J GARNIER AND K SÖLNA, *Coupled paraxial wave equations in random media in the white-noise regime*, The Annals of Applied Probability, 19 (2009), pp. 318–346. [2](#), [4](#)
- [17] ———, *Fourth-moment analysis for wave propagation in the white-noise paraxial regime*, Archive for Rational Mechanics and Analysis, 220 (2016), pp. 37–81. [2](#)
- [18] ———, *Imaging through a scattering medium by speckle intensity correlations*, Inverse Problems, 34 (2018), p. 094003. [2](#)
- [19] ———, *Speckle memory effect in the frequency domain and stability in time-reversal experiments*, arXiv:2201.05558, (2022). [2](#)
- [20] C GOMEZ AND O PINAUD, *Fractional white-noise limit and paraxial approximation for waves in random media*, Archive for Rational Mechanics and Analysis, 226 (2017), pp. 1061–1138. [2](#)
- [21] IS GRADSTEIN AND IM RYZHIK, *Tables of integrals and functions*, Academic Press, New York, 1980. [5](#)
- [22] A HASEGAWA AND F TAPPERT, *Transmission of stationary nonlinear optical pulses in dispersive dielectric fibers. I. Anomalous dispersion*, Applied Physics Letters, 23 (1973), pp. 142–144. [1](#)
- [23] A ISHIMARU, *Wave Propagation and Scattering in Random Media*, IEEE Press, 1997. [1](#)

- [24] O KOROTKOVA AND I TOSELLI, *Non-classic atmospheric optical turbulence*, Applied Sciences, 11 (2021), p. 8487. [2](#)
- [25] HJ KUSHNER, *Approximation and Weak Convergence Methods for Random Processes, with Applications to Stochastic Systems Theory*, The MIT Press, Cambridge, 1984. [8](#)
- [26] MA LEONTOVICH AND VA FOCK, *Solution of the problem of propagation of electromagnetic waves along the earth's surface by the method of parabolic equation*, J. Phys. USSR, 10 (1946), pp. 13–23. [1](#)
- [27] BL MADHAVAN, H DENEKE, J WITTHUHN, AND A MACKE, *Multiresolution analysis of the spatiotemporal variability in global radiation observed by a dense network of 99 pyranometers*, Atmospheric Chemistry and Physics, 17 (2017), pp. 3317–3338. [2](#)
- [28] BB MANDELBROT AND JW VAN NESS, *Fractional brownian motions, fractional noises and applications*, SIAM review, 10 (1968), pp. 422–437. [7](#)
- [29] R MARTY, *Théorème limite pour une équation différentielle à coefficient aléatoire à mémoire longue*, C. R. Acad. Sci. Paris, Ser. I , 338 (2004), pp. 167–170. [6](#)
- [30] R MARTY AND K SØLNA, *A general framework for waves in random media with long-range correlations*, Ann. Applied Probability, 21 (2011), pp. 115–139. [6](#)
- [31] G PAPANICOLAOU, L RYZHIK, AND K SØLNA, *Self-averaging from lateral diversity in the Itô–Schrödinger equation*, Multiscale Modeling & Simulation, 6 (2007), pp. 468–492. [2](#), [10](#)
- [32] K SØLNA, *Acoustic pulse spreading in a random fractal*, SIAM Journal on Applied Mathematics, 63 (2003), pp. 1764–1788. [2](#)
- [33] FD TAPPERT, *The parabolic approximation method*, in Wave propagation and underwater acoustics, vol. 70 of Lecture notes in physics, Springer, 1977, pp. 224–287. [1](#)
- [34] VI TATARSKII, *Waves Propagation in a Turbulent Medium*, McGraw-Hill, 1961. [1](#)
- [35] CY YOUNG, A ISHIMARU, AND LC ANDREWS, *Two-frequency mutual coherence function of a Gaussian beam pulse in weak optical turbulence: an analytic solution*, Applied optics, 35 (1996), pp. 6522–6526. [1](#)
- [36] A ZILBERMAN, E GOLBRAIKH, AND NS KOPEIKA, *Propagation of electromagnetic waves in Kolmogorov and non-Kolmogorov atmospheric turbulence: three-layer altitude model*, Applied optics, 47 (2008), pp. 6385–6391. [2](#)